NAVAL POSTGRADUATE SCHOOL
Monterey, California

THESIS

ADVANCED APPLICATIONS FOR 0.53 μm LASER LIGHT

by

W. David Jones

June 2001

Thesis Advisor: William L. Kruer
Second Reader: William B. Colson

Approved for public release; distribution is unlimited

REPORT DOCUMENTATION PAGE			Form Approved OMB No. 0704-0188
Public reporting burden for this collection of information is estimated to average 1 hour per response, including the time for reviewing instruction, searching existing data sources, gathering and maintaining the data needed, and completing and reviewing the collection of information. Send comments regarding this burden estimate or any other aspect of this collection of information, including suggestions for reducing this burden, to Washington headquarters Services, Directorate for Information Operations and Reports, 1215 Jefferson Davis Highway, Suite 1204, Arlington, VA 22202-4302, and to the Office of Management and Budget, Paperwork Reduction Project (0704-0188) Washington DC 20503.			
1. AGENCY USE ONLY *(Leave blank)*	**2. REPORT DATE** June 2001	**3. REPORT TYPE AND DATES COVERED** Master's Thesis	
4. TITLE AND SUBTITLE: Title (Mix case letters) Advanced Applications for 0.53 μm Laser Light			**5. FUNDING NUMBERS**
6. AUTHOR(S) W. David Jones			
7. PERFORMING ORGANIZATION NAME(S) AND ADDRESS(ES) Naval Postgraduate School Monterey, CA 93943-5000			**8. PERFORMING ORGANIZATION REPORT NUMBER**
9. SPONSORING / MONITORING AGENCY NAME(S) AND ADDRESS(ES) N/A			**10. SPONSORING / MONITORING AGENCY REPORT NUMBER**
11. SUPPLEMENTARY NOTES The views expressed in this thesis are those of the author and do not reflect the official policy or position of the Department of Defense or the U.S. Government.			
12a. DISTRIBUTION / AVAILABILITY STATEMENT Approved for public release; distribution is unlimited			**12b. DISTRIBUTION CODE**

13. ABSTRACT ***(maximum 200 words)***

Use of the National Ignition Facility with green light as the laser output is an intriguing option for advanced applications ranging from inertial fusion to production of compact x-ray sources. Particular attention is given to the potential use of 0.53 μm light to produce a high-energy x-ray source. This application requires the efficient generation of high-energy electrons which can subsequently produce high-energy x-rays as they transport into gold or other high Z wall. One- and two-dimensional computer simulations are used to explore high-energy electron generation by intense 0.53 μm laser light in a plasma with density near one-quarter the critical density. Significant absorption is shown to occur into high-energy electrons with an effective temperature which is reduced by the development of ion fluctuations. The results compare favorably with some recent experiments using 0.53 μm light.

14. SUBJECT TERMS High intensity Lasers, Laser-Plasma Coupling, National Ignition Facility, Fusion, Computer Simulations			**15. NUMBER OF PAGES** 55
			16. PRICE CODE
17. SECURITY CLASSIFICATION OF REPORT Unclassified	**18. SECURITY CLASSIFICATION OF THIS PAGE** Unclassified	**19. SECURITY CLASSIFICATION OF ABSTRACT** Unclassified	**20. LIMITATION OF ABSTRACT** UL

NSN 7540-01-280-5500

Standard Form 298 (Rev. 2-89)
Prescribed by ANSI Std. 239-18

THIS PAGE INTENTIONALLY LEFT BLANK

Approved for public release; distribution is unlimited

ADVANCED APPLICATIONS FOR 0.53μm LASER LIGHT

W. David Jones
Captain, United States Army
B.S., North Carolina State University, 1990

Submitted in partial fulfillment of the
requirements for the degree of

MASTER OF SCIENCE IN PHYSICS

from the

NAVAL POSTGRADUATE SCHOOL
June 2001

Author: _____
W. David Jones

Approved by: _____
William L. Kruer, Thesis Advisor

_____
William B. Colson, Co-Advisor

_____
William Maier, Chairman
Department of Physics

THIS PAGE INTENTIONALLY LEFT BLANK

ABSTRACT

Use of the National Ignition Facility with green light as the laser output is an intriguing option for advanced applications ranging from inertial fusion to production of compact x-ray sources. Particular attention is given to the potential use of 0.53 μm light to produce a high-energy x-ray source. This application requires the efficient generation of high-energy electrons which can subsequently produce high-energy x-rays as they transport into gold or other high Z wall. One- and two-dimensional computer simulations are used to explore high-energy electron generation by intense 0.53 μm laser light in a plasma with density near one-quarter the critical density. Significant absorption is shown to occur into high-energy electrons with an effective temperature which is reduced by the development of ion fluctuations. The results compare favorably with some recent experiments using 0.53 μm light.

THIS PAGE INTENTIONALLY LEFT BLANK

TABLE OF CONTENTS

THIS PAGE INTENTIONALLY LEFT BLANK

LIST OF FIGURES

THIS PAGE INTENTIONALLY LEFT BLANK

LIST OF TABLES

THIS PAGE INTENTIONALLY LEFT BLANK

ACKNOWLEDGMENTS

- First and foremost, I want to acknowledge my family. Without the support of my wife, Sandra, I would never have made it to this point in my Army career. My daughters, Meghan and Corrie, have endured long hours with mom wondering why dad is spending so much time away from them. Without a doubt, these two years have been hard on them, and I have to thank them for being there for me.

- Second, I want to acknowledge all of the teachers I have had the pleasure of having while at the Naval Postgraduate School. They put in many long hours to ensure top quality education. Without their dedication and long hours at work, I wouldn't have received the instruction to make this thesis possible.

- Third, I want to acknowledge Dr. Dan Gordon, NRL, the creative writer for the program, Turbowave, which is extensively used throughout the simulations portion of this thesis. Without his help, certainly the simulations would not have worked.

- Fourth, I want to acknowledge Professor Warren Mori, Dr. Chuang Ren, and Dr. Frank Tsung of the Plasma Physics Department at the University of California, Los Angeles. Their help ensured the overall success of the simulations. And they have the World's best orange juice. No wonder there are lots of smart folks there.

- Fifth, I'd like to thank the good people at Lawrence Livermore National Labs. The tours of the labs and the National Ignition Facility helped spark my initial interest into this branch of physics.

- Sixth, I'd like to thank Dr. William L. Kruer, my thesis advisor and friend, for the many patient hours running simulations with me, helping me to understand the results and graphs, and spending the time to ensure I knew what I was talking about during the thesis presentation and the Anomalous Absorption Conference. You're an extraordinary man whom I'm proud to know.

- Finally, I'd like to publicly acknowledge God. As the sovereign Creator of the universe, He knows much more about plasma than I ever will, but He has given me a glimpse into the possibilities that this branch of science promises for the future.

- The plasma simulation capability at NPS and the collaboration with UCLA were made possible by support from DTRA to investigate laser-plasma x-ray sources under NPS Contract RPH4J.

THIS PAGE INTENTIONALLY LEFT BLANK

I. INTRODUCTION

The purpose of this thesis is to present computer simulations of laser – plasma interactions. Specifically, I intend to examine how much energy from the input laser is converted into heated electrons, and what the energies of those electrons are. The production of high-energy electrons depends on how efficiently a uniform plasma absorbs 0.53 μm green laser light.

Numerous ways have been proposed to create a viable source of sustained fusion using a large number of high-intensity lasers to compress and heat a capsule containing a small quantity of deuterium and tritium. At present, researchers are concentrating on two major avenues, namely direct drive and indirect drive. The goal for each method is the same: to create more sustainable output power than the quantity input. The major difference is that direct drive involves focusing all the individual laser beams directly onto the capsule and heating the deuterium – tritium target very uniformly. Indirect drive involves shining the individual laser beams onto a small cylinder of high atomic weight material, usually gold, which forms a plasma. This plasma emits x-rays. These x-rays then cause the deuterium – tritium target to compress and heat until fusion is achieved. Figures 1 and 2 show the much-simplified view of each process.

Although sustained fusion is a noteworthy goal, the laser intensity must be lower than the values I have used in this project to negate producing high-energy electrons and x-rays. I am keeping the intensity high to produce these generally undesired laser-plasma interaction effects.

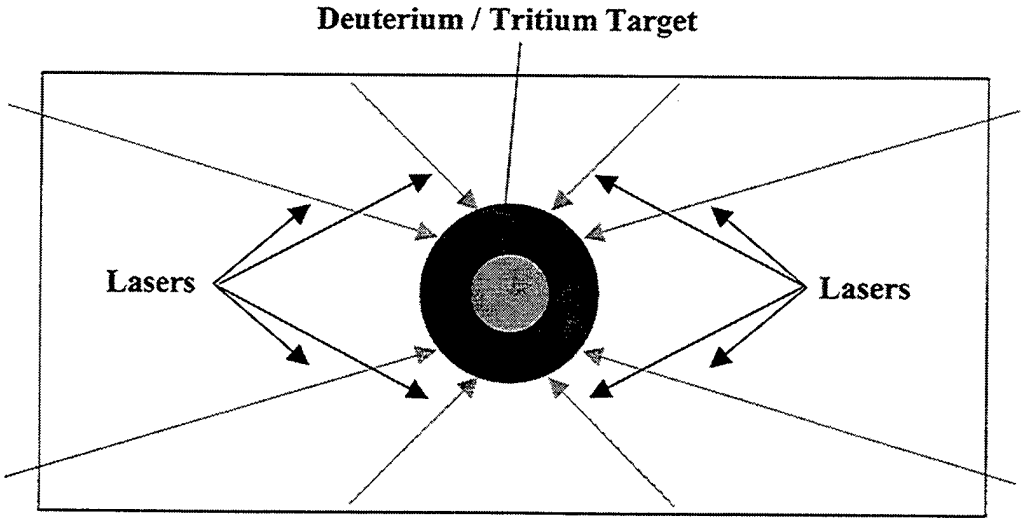

Figure 1. Direct Drive Fusion.

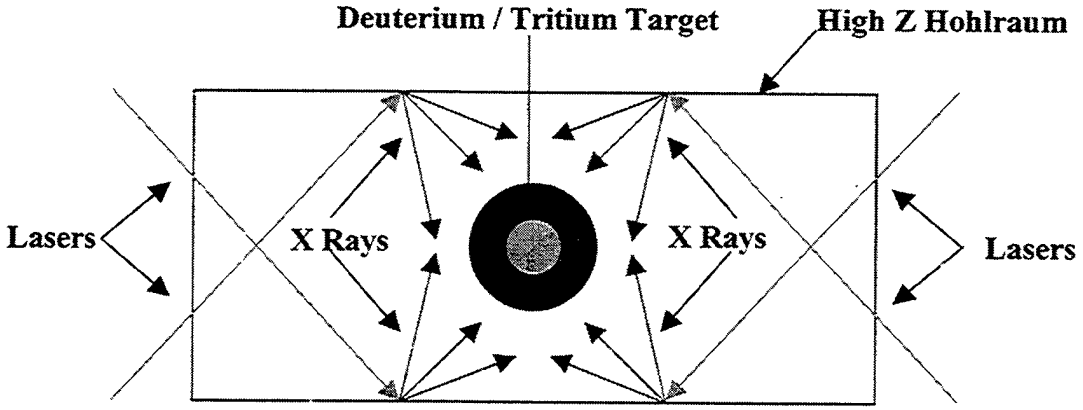

Figure 2. Indirect Drive Fusion

A. UNDERSTANDING PLASMAS AND PLASMA COMPUTER SIMULATIONS

A plasma is basically a semi-neutral collection of charged particles that exhibit collective behavior. Plasmas exist all around us, and actually comprise the largest

fraction of matter in the universe. Without plasmas, it is safe to say that life as we know it would not exist on the earth. We have learned to harness plasmas in many useful ways, such as low-consumption fluorescent lights and cathode-ray tubes. Scientists have been researching ways to make further uses, and it is a goal to use plasmas to power fusion reactors with the hope of eliminating the world's dependence on less efficient means to generate electricity. We are still a long way off from such a noble goal.

Plasmas are described on a large scale by their temperatures and densities and on a small scale by the statistical positions and velocities of the particles. Given the large number of particles, a statistical approach is used and provides accurate information. Plasmas as a whole also display a wide range of interesting phenomena, including waves (electron plasma waves and ion acoustic waves), instabilities (Raman and Brillouin Scattering are the most commonly studied for inertial fusion), damping (Landau damping for example), and dispersion of incident radiation. Some of these phenomena will be discussed since they directly affect the usefulness of plasma in the problem of power generation.

One can describe a plasma as a large number of charges in a system in which the particles are coupled together by way of their electric and magnetic fields. Attempting to study the behavior of each particle would be a monumental task far beyond the reach of all but the most sophisticated, powerful computers in the world. Even they can not handle a large plasma, since a single mole of any element would contain approximately 6 x 10^{23} molecules. A singly charged plasma would therefore contain twice as many particles (ions and electrons). The particles would also be randomly distributed, and the net charge of the plasma would effectively be zero. Computer random number generators

would provide a sense of electric field irregularities found in nature based on the number and position of particles. Random number generators would also produce velocities based on ion and electron temperatures, direction vectors, and displacements to simulate the initial plasma conditions. To simplify the problem, the temperature would have to be sufficiently high to assure a nearly collisionless plasma. If collisions were considered as part of the plasma condition, then the calculations would exceed even the most powerful computers available today. To mitigate the problem, we choose a much smaller number of plasma particles that most desktop computers can handle. Now we enter the realm of computer simulations of plasmas. More than 10 years ago (around 1990), scientists had very few computers available that could handle large quantities of data and that could perform the enormous number of calculations necessary to assure statistically accurate pictures of plasma behavior. Now the average computer available on the open market can handle the types of interesting problems typically encountered. Systems are currently available that can handle a fairly large number of particles and that provide a reasonable solution to a complex problem. As the technology of computers advances, systems with multiple processors and large memory cores will be able to handle larger and larger numbers of particles in codes and provide even more realistic solutions.

For this problem, assume that the plasma can be decomposed into two distinct electric fields, $\mathbf{E}_1$ and $\mathbf{E}_2$. $\mathbf{E}_1$ has a spatial variation much less than the electron Debye Length, λ_{DEBYE}. The Debye Length is characterized by the length of shielding that an electron (or ion) provides for a surrounding number of charges. It is determined by

$$\lambda_{DEBYE} = (\varepsilon_0 K T_{electron} / n e^2)^{1/2}$$

where ε_0 is the permittivity of free space, $\mathbf{T_{electron}}$ is the electron plasma temperature, **n** is the density of the plasma, **K** is a constant, and **e** is the basic electronic charge. This shielding is an important effect in keeping the plasma electrically neutral. The field of an individual charge is shielded out by the surrounding charges over the Debye Length. $\mathbf{E_1}$ is essentially the fluctuating field due to multiple, random collisions among the vast number of plasma particles. $\mathbf{E_2}$, on the other hand, varies on a scale larger than the Debye Length and represents the forces due to the average collective motion of all of the charges. Fortunately, we can neglect the effects of $\mathbf{E_1}$ because collisional behavior is negligible for a large number of electrons within a given Debye Sphere. Another way of sufficing the plasma condition is by saying that the number of particles in a Debye Sphere must be much, much greater than one ($N_D >> 1$).

Particles within a plasma have a wide distribution of velocity. It is necessary to apply statistics to determine the average velocity and therefore the temperature. Often one has a Maxwellian distribution of velocities. Plasma temperatures are generally given in terms of energy, not in degrees Kelvin. The conversion factor for temperature is

1 electron – volt = 11,594 K

With rounding to three significant digits, it is generally accepted that 1 eV ≅ 11,600 K.

Plasmas are composed of charged particles, as noted before. The masses of the ions are at a minimum of 1,836 times the masses of the electrons for a simple hydrogen plasma. With higher Z materials, the ions are made much heavier. The effect is that the ions are not moved very much when electrons bounce into them. Therefore, little energy is exchanged, so that there are effectively two different temperatures present: the ion

temperature (T_i) and the electron temperature (T_e). Each species can exhibit its own thermal equilibrium.

B. COMPUTER SIMULATIONS OF PLASMAS

Plasmas can be readily simulated using computer codes in a variety of languages such as MATLAB, FORTRAN, and C++. Computer codes provide a powerful approach to study the non-linear effects of laser – plasma interactions. Much of the plasma's behavior is non-linear, so the computer is the best resource to use. The codes allow us to simulate the behavior of a limited number of representative particles and apply the simulation to the whole plasma. One must use a sufficiently large number of particles to statistically approximate what is actually happening inside the real plasma. However, it is also possible to overload a computer's available memory resources by choosing too large a number. It is also necessary to incorporate the correct time step in the code for reliable results. For example, the Courant Condition must be satisfied when solving Maxwell's equations. The Courant Condition relates the step sizes for both time and the grid size. The Courant Condition in mathematical form looks like

$$(c\,\Delta t)^2 \left[(1 / \Delta x)^2 + (1 / \Delta y)^2 \right] < 1$$

where c is the speed of light, Δt is the time step, Δx is the step size in the x-direction, and Δy is the step size in the y-direction. One must also take care to choose step and time sizes sufficiently small to resolve the highest frequency behavior in the problem.

Since computers can't actually execute derivatives of functions and solve them directly, it is necessary to use numerical finite difference methods. The simplest case to

solve, but one that provides an enormous amount of information, is the one-dimensional problem using just Poisson's Equation:

$$\varepsilon_0 \frac{\partial \mathbf{E}}{\partial \mathbf{x}} = (\mathbf{e})(\mathbf{n}_{ion} - \mathbf{n}_{electron})$$

In this equation, ε_0 is the permittivity of free space, **E** is the electric field, **e** is the basic electronic charge, $\mathbf{n}_{ion}$ is the ion charge density, and $\mathbf{n}_{electron}$ is the electron density. In using the finite difference method, we use

$$\frac{\partial \mathbf{E}}{\partial \mathbf{x}} = \frac{\mathbf{E}_{(i+1)} - \mathbf{E}_{(i)}}{\delta}$$

where the subscript, **i**, denotes the grid location and δ is the cell size. In the simplest case, variations occur only in one dimension and periodic boundary conditions are used, effectively "wrapping around" the fields once they reach the end of the simulated plasma. Figure 3 shows the cycle the code implements throughout the simulation.

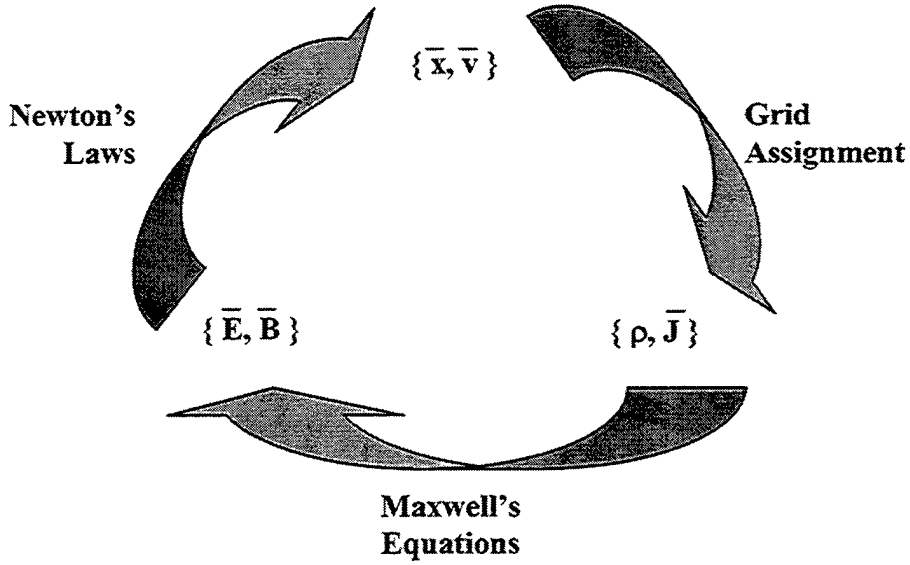

Figure 3. Particle Simulation Cycle. Note: $\bar{x}$ is position, $\bar{v}$ is velocity, ρ is charge density, $\bar{J}$ is current, $\bar{E}$ is the electric field, and $\bar{B}$ is the magnetic field.

To assign the charge density, ρ, and position, x, to the grid, the length of the plasma is divided into "cells," determined by the user. The particles are then assigned to the linear "grid;" the grid is divided into an integer number of units, with the cell size, δ, equal to one. The linear grid starts with one and increases by integer values to the right, as in an ordinary number line. Beyond the last grid point, the code automatically sends the particles back around to the first grid point, thus "wrapping" the particles around, which accounts for the periodic boundary conditions. The entire charge is not assigned to a specific grid; instead, each particle's charge is shared between adjacent grids. Figure 4 demonstrates how charge sharing occurs in the program.

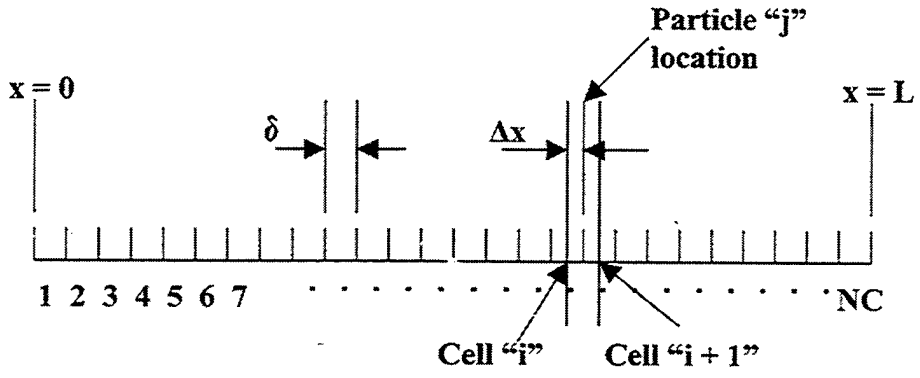

Figure 4. Charge Sharing Used in Plasma Simulation Codes.

For a charge located a distance Δx to the right of grid point i, the following equations govern charge sharing:

$$\Delta\rho(i) = (q)(1 - \Delta x)$$

$$\Delta\rho(i+1) = (q)(\Delta x)$$

where $\Delta\rho$ is the change in charge density, q is the charge, and Δx is the step size.

Figure 5 shows charge sharing in more detail.

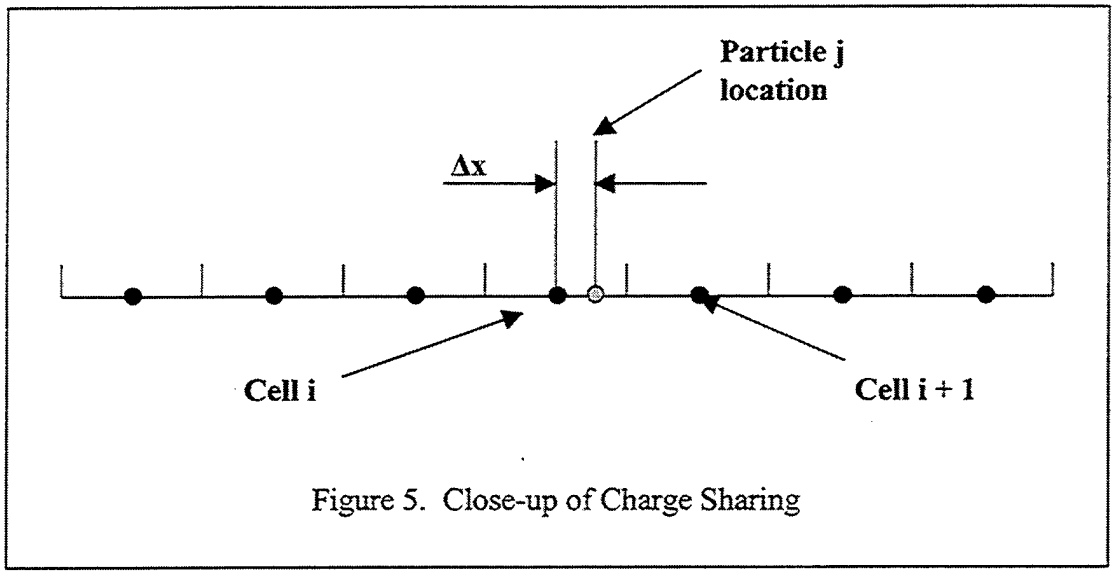

Figure 5. Close-up of Charge Sharing

The force on a particle is generated using a similar technique. For a given particle, the force is calculated as

$$F = (q)(E_{(i)})(1 - \Delta x) + (q)(E_{(i+1)})(\Delta x)$$

Where q is charge, E is the electric field at position i, and Δx is the step size. The code assumes no external magnetic fields. This allows the position and velocity to be updated by Δt in time using

$$v^{n+\frac{1}{2}} = v^{n-\frac{1}{2}} + F^{n} \cdot \Delta t$$

$$x^{n+1} = x^{n} + v^{n+\frac{1}{2}} \cdot \Delta t$$

where v is velocity, F is force, x is position, and Δt is the time step. The superscripts define the time step of the program. By using this algorithm, one effectively achieves second-order accuracy.

The cycle continues until the end time is reached using a sufficiently small time step to resolve the plasma oscillations. Using the electrostatic case, the electron plasma frequency, ω_{PLASMA}, is the highest frequency that one could expect to encounter. It is equal to

$$\omega_{PLASMA}^2 = \frac{n e^2}{m \varepsilon_0}$$

where **n** is the density, **e** is the basic electronic charge, **m** is the mass of an electron, and ε_0 is the permittivity of free space. A time step must be on the order of, or less than, 0.2 / ω_{PLASMA} in order to resolve the high frequency effects. The grid size is usually chosen to be about the Debye Length. Choosing a grid size that is too many Debye Lengths introduces a numerical instability called aliasing.

C. OTHER PROGRAMMING CONSIDERATIONS

I modified a simple one-dimensional, electrostatic particle code in MATLAB to demonstrate its usefulness. The program uses a random number generator to establish the initial particle positions. Such a practice can introduce noise into the code that can hide some non-linear behaviors. The code is written to be "quiet" near the low amplitude regions where this effect can be the most damaging. One can study many interesting plasma effects even with this simple code.

II. DEMONSTRATION OF ONE-DIMENSIONAL MATLAB CODE

As a simple example, I used the MATLAB code to illustrate electron heating by large amplitude electron plasma waves. A spatially homogeneous electric field oscillating with frequency near the electron plasma frequency (ω_{PLASMA}) drives these waves and the accompanying ion fluctuations unstable. The electron plasma waves grow to a large amplitude and accelerate and heat the electrons. I show the simulation results in the following figures. The left hand side shows the electron phase space (velocity versus position) and the right hand side shows the distribution function (number of electrons versus velocity). The last figure (Figure 6u) shows the time evolution of the various energies.

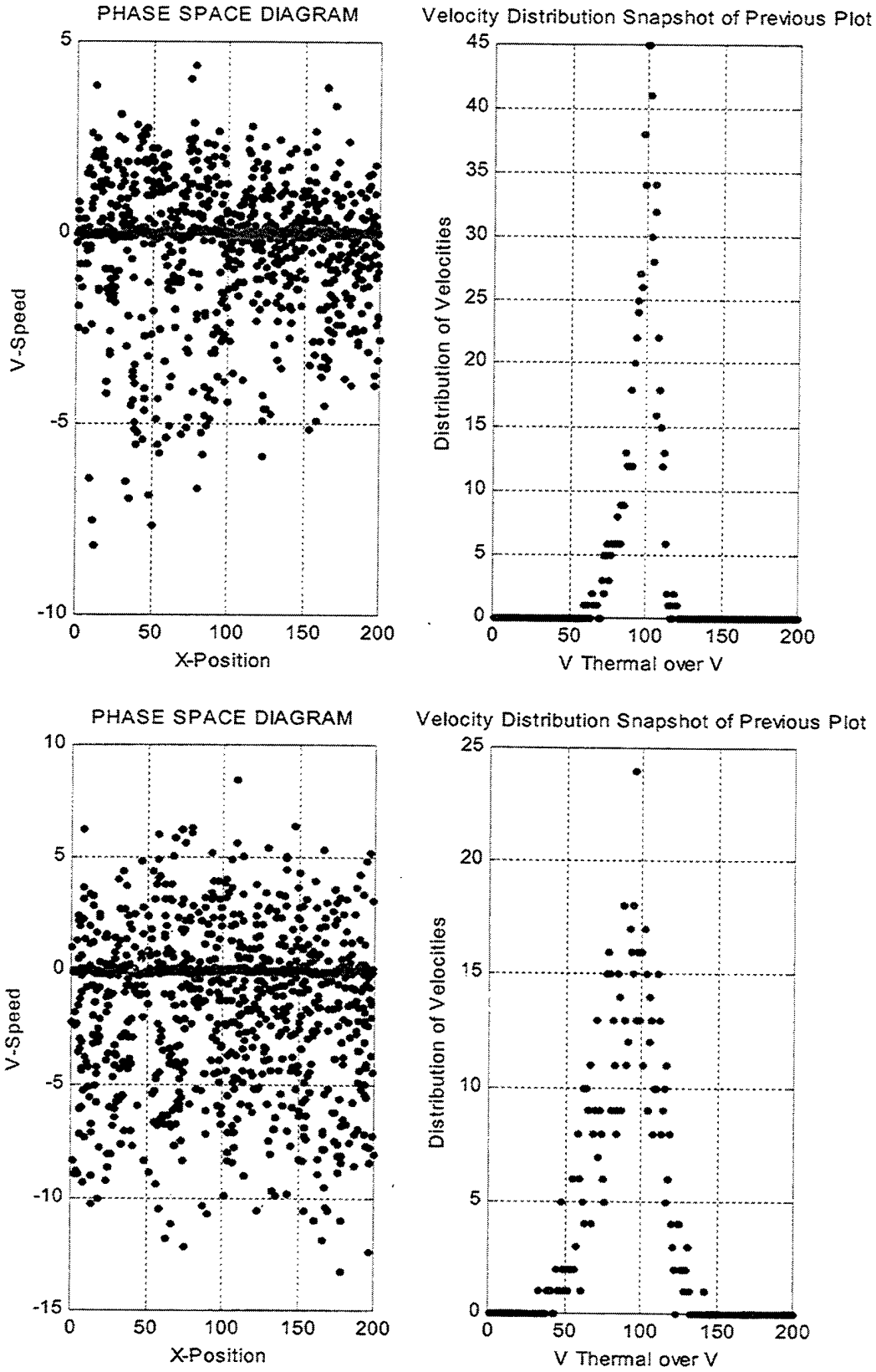

Figures 6a and 6b. Phase Space and Velocity Distributions at times 50 and 100

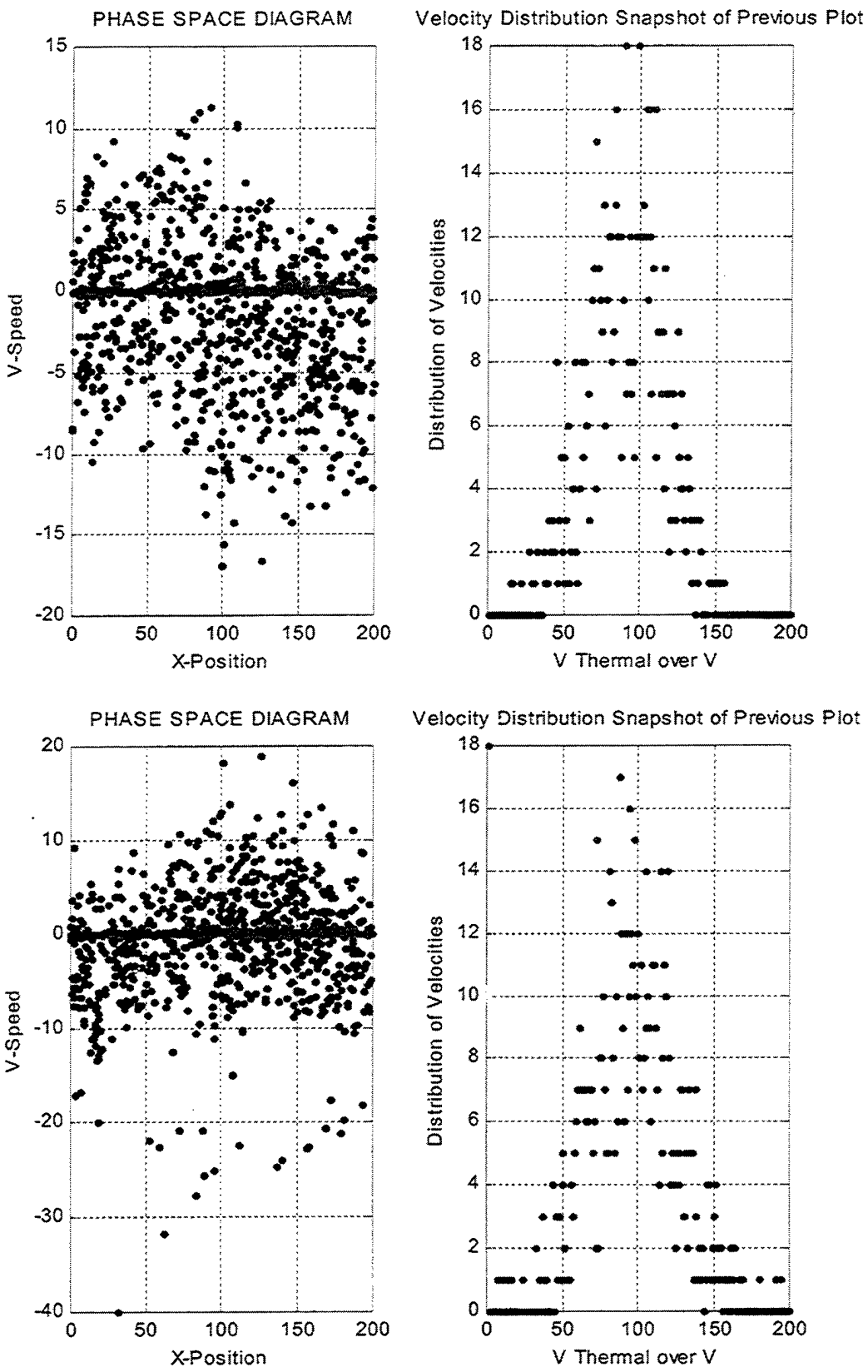

Figures 6c and 6d. Phase Space and Velocity Distributions at times 150 and 200

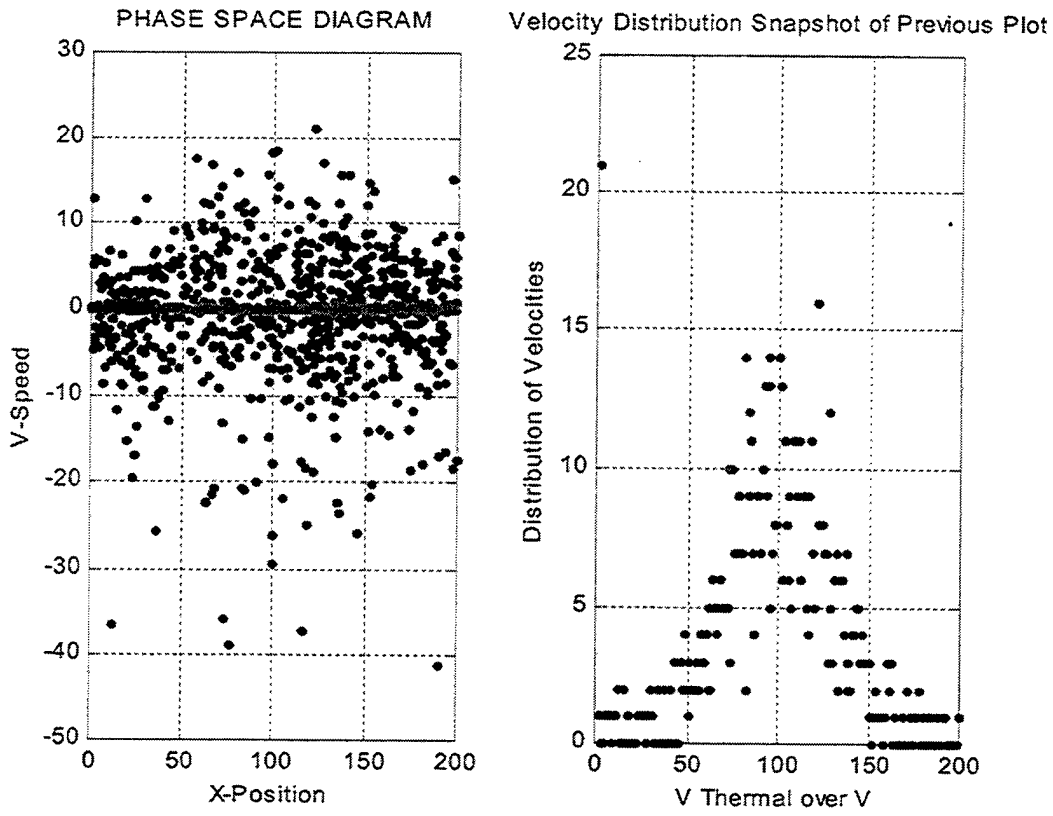

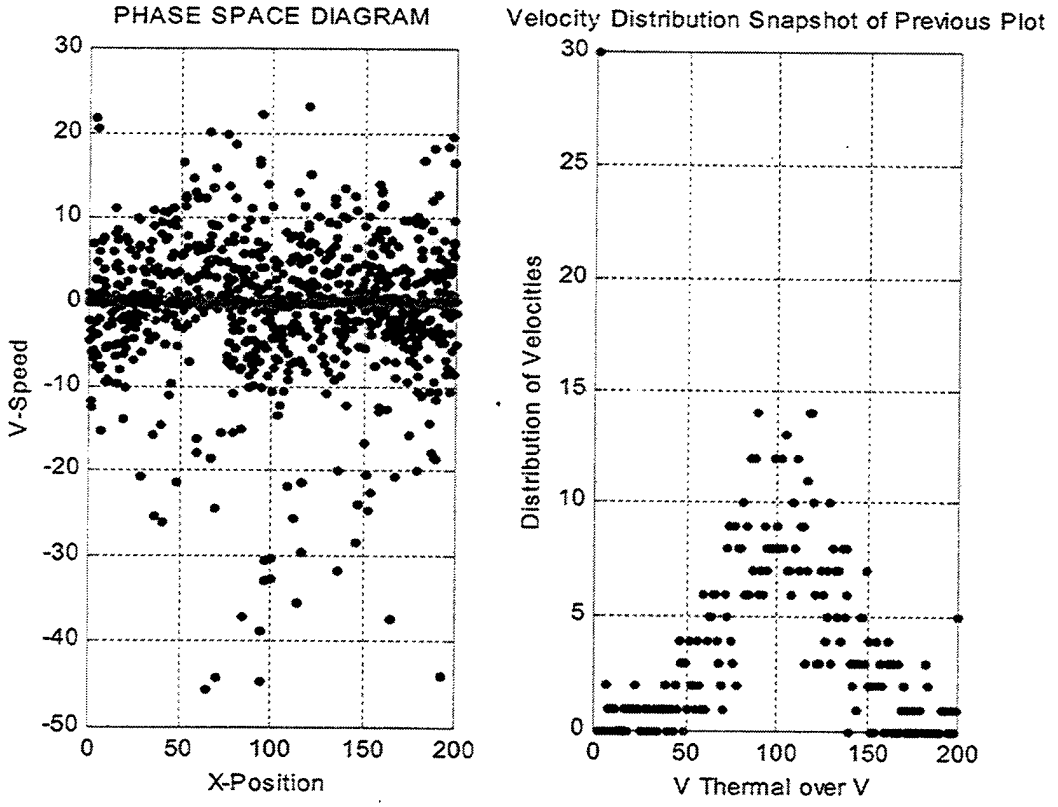

Figures 6e and 6f. Phase Space and Velocity Distributions at times 250 and 300

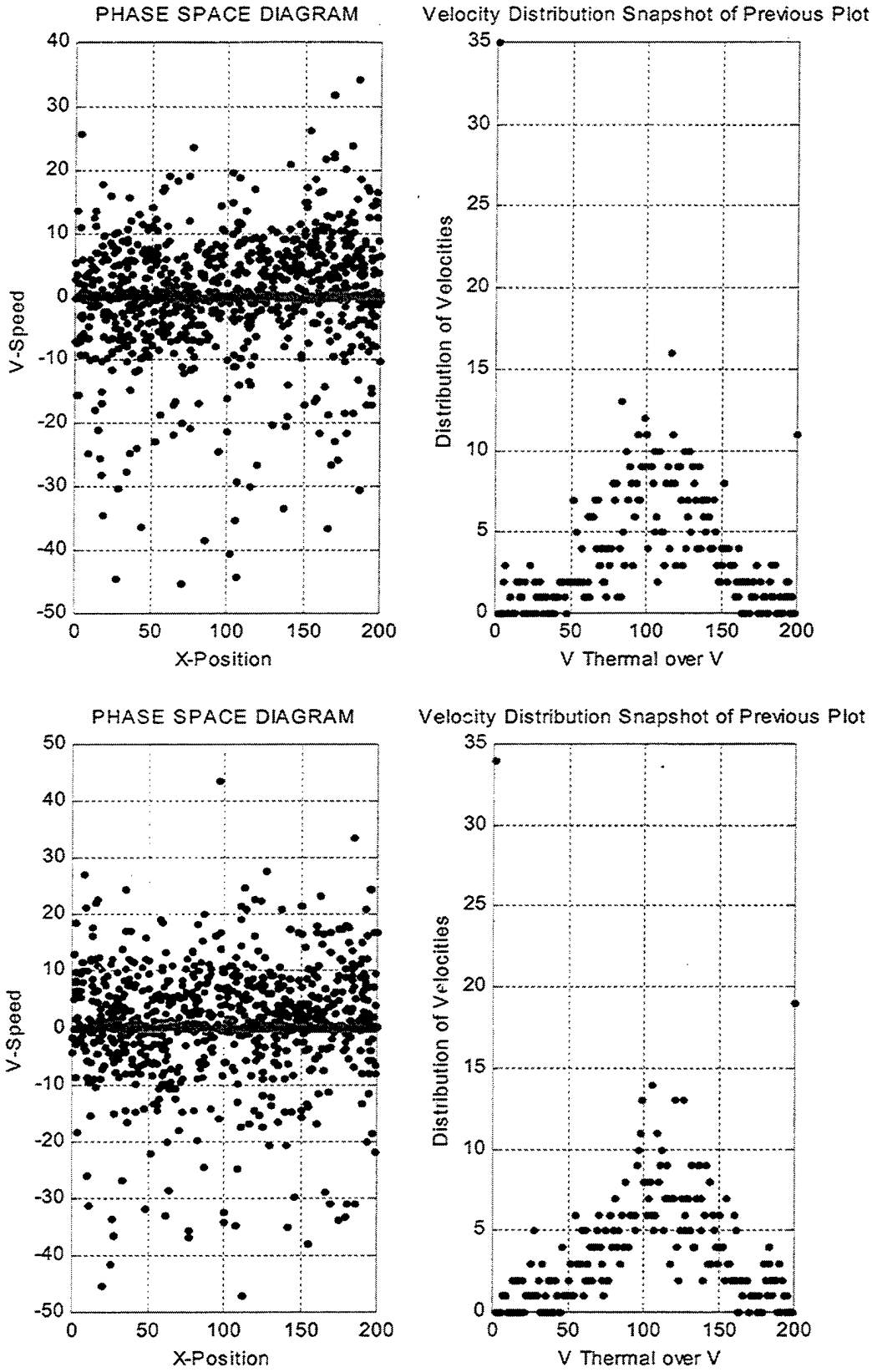

Figures 6g and 6h. Phase Space and Velocity Distributions at times 350 and 400

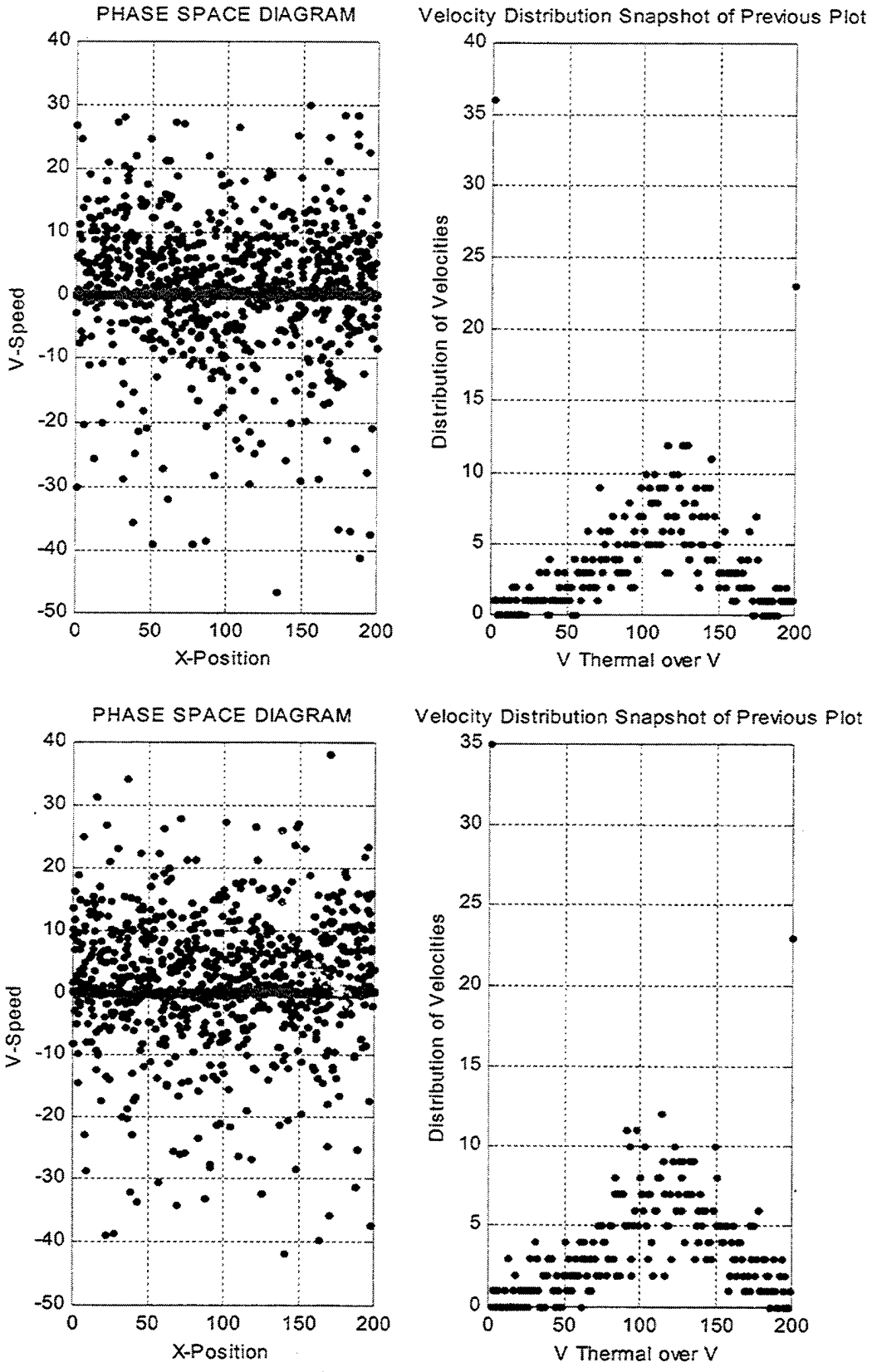

Figures 6i and 6j. Phase Space and Velocity Distributions at times 450 and 500

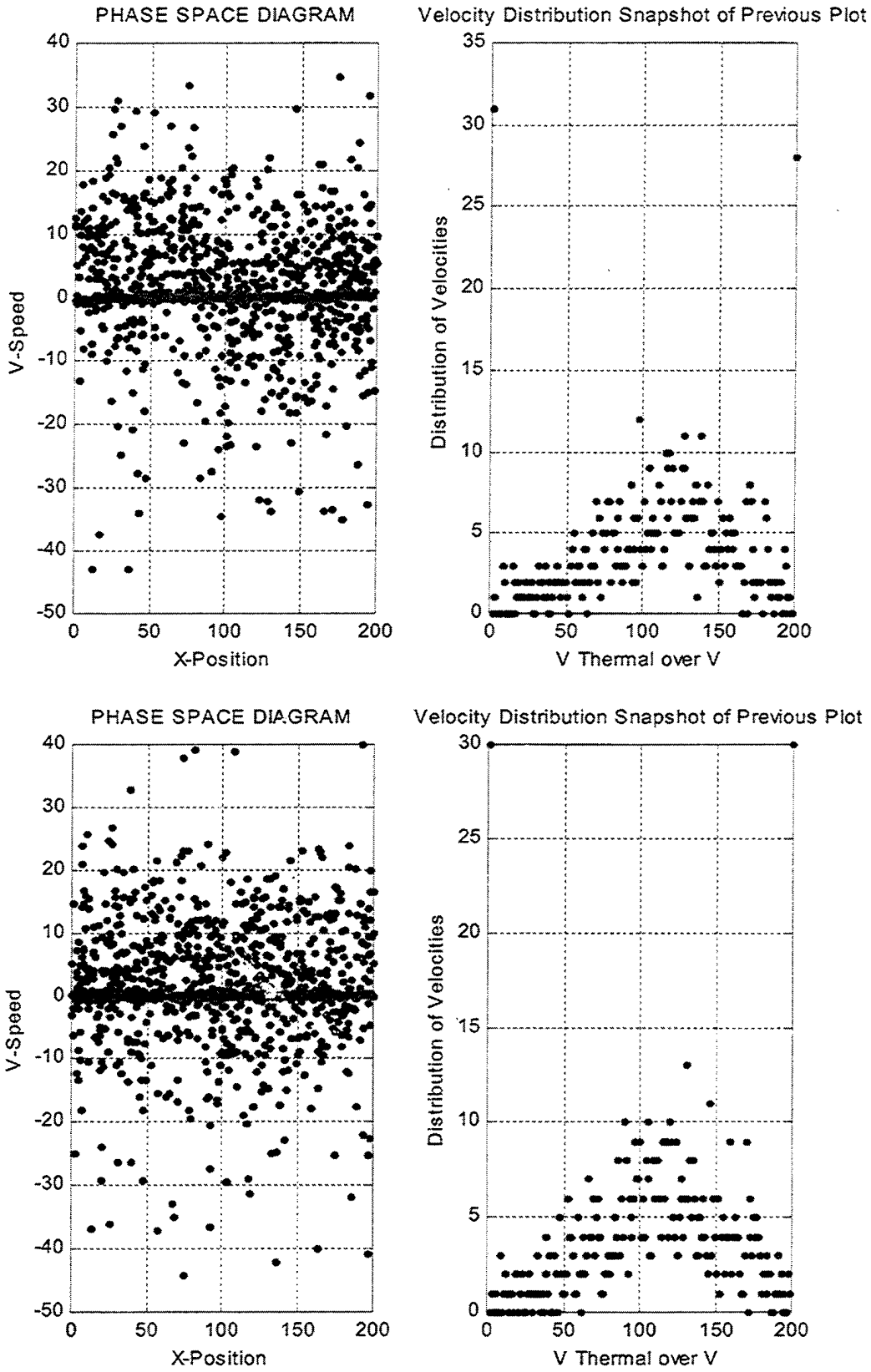

Figures 6k and 6l. Phase Space and Velocity Distributions at times 550 and 600

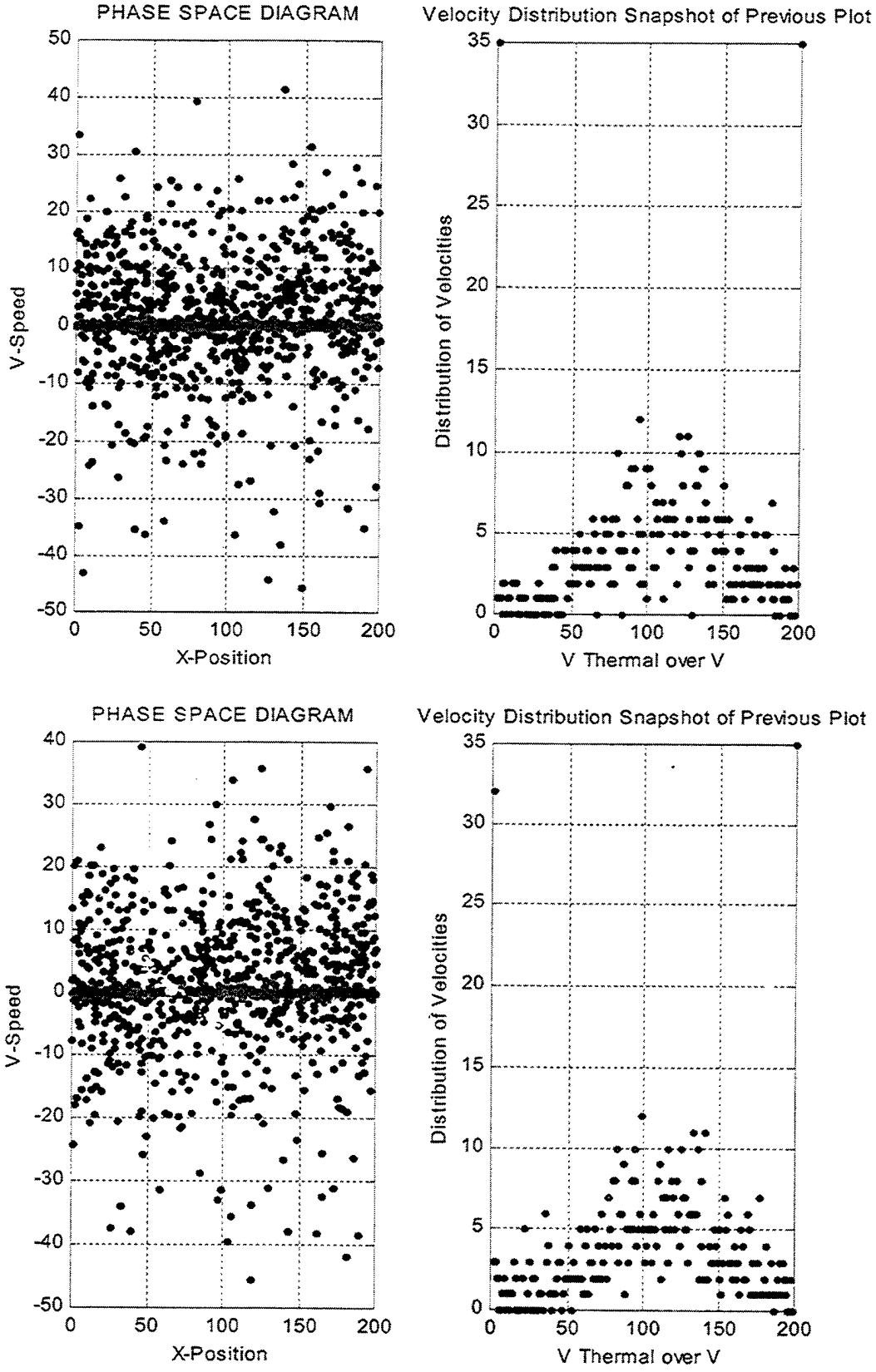

Figures 6m and 6n. Phase Space and Velocity Distributions at times 650 and 700

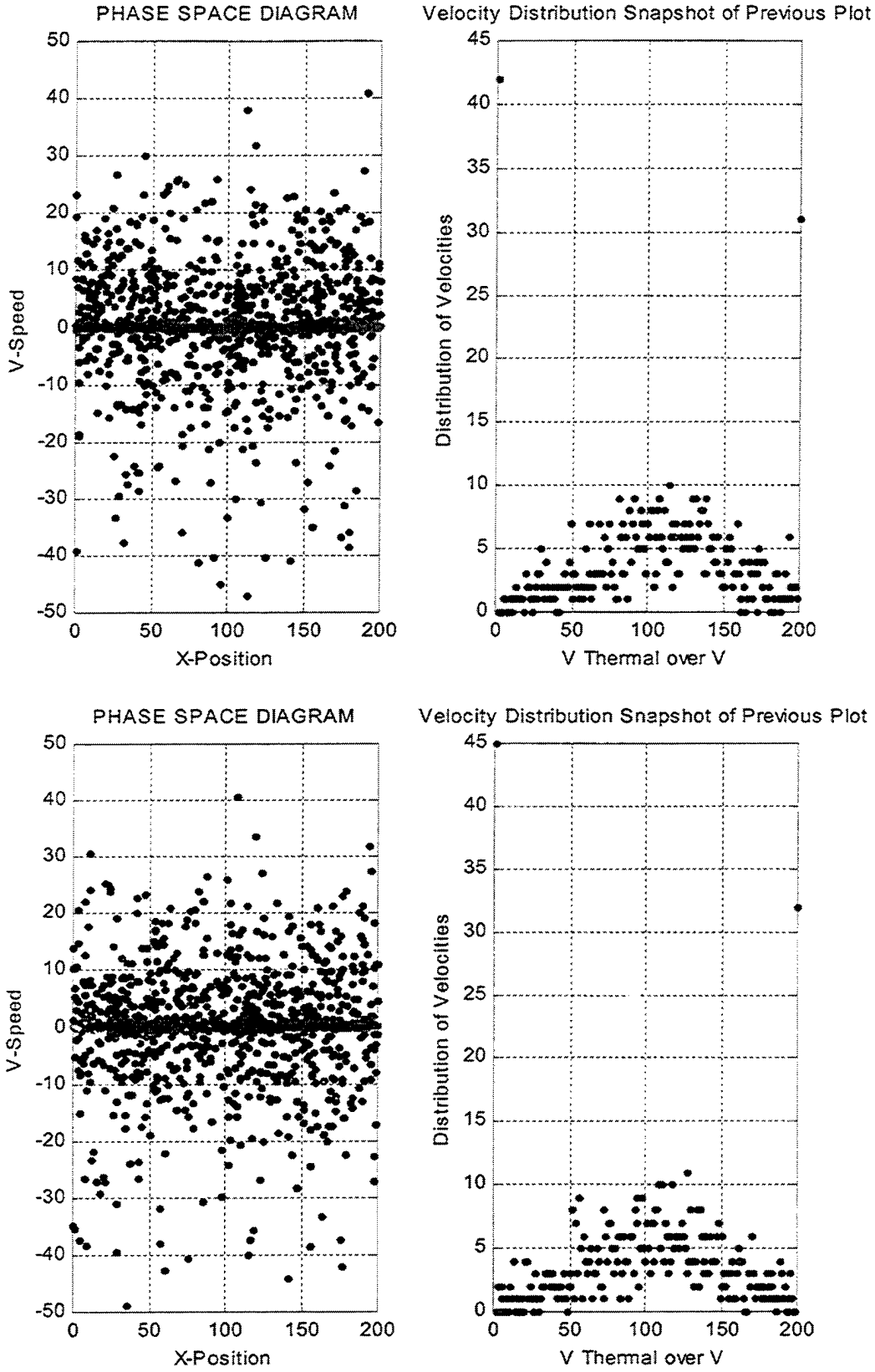

Figures 6o and 6p. Phase Space and Velocity Distributions at times 750 and 800

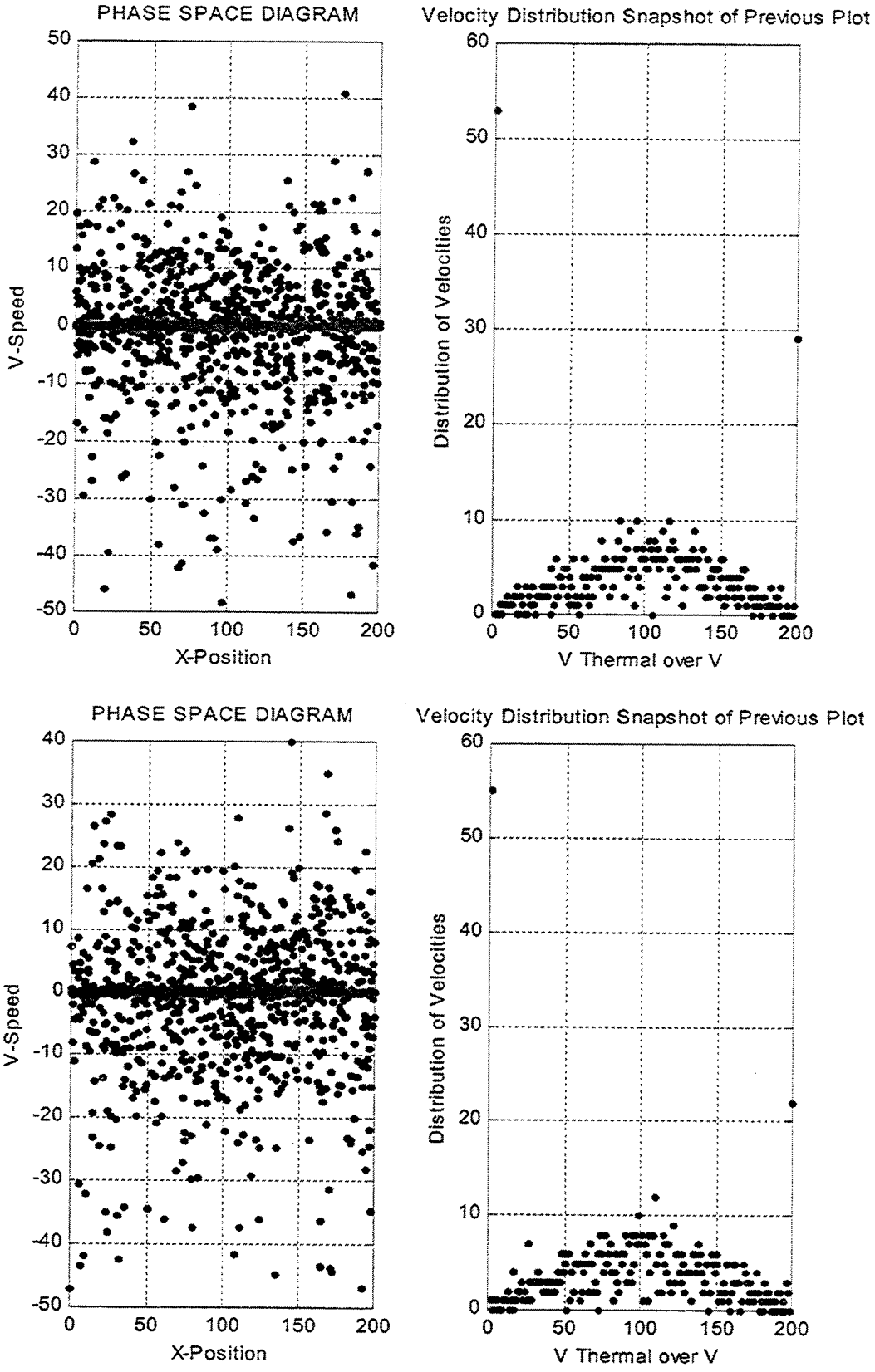

Figures 6q and 6r. Phase Space and Velocity Distributions at times 850 and 900

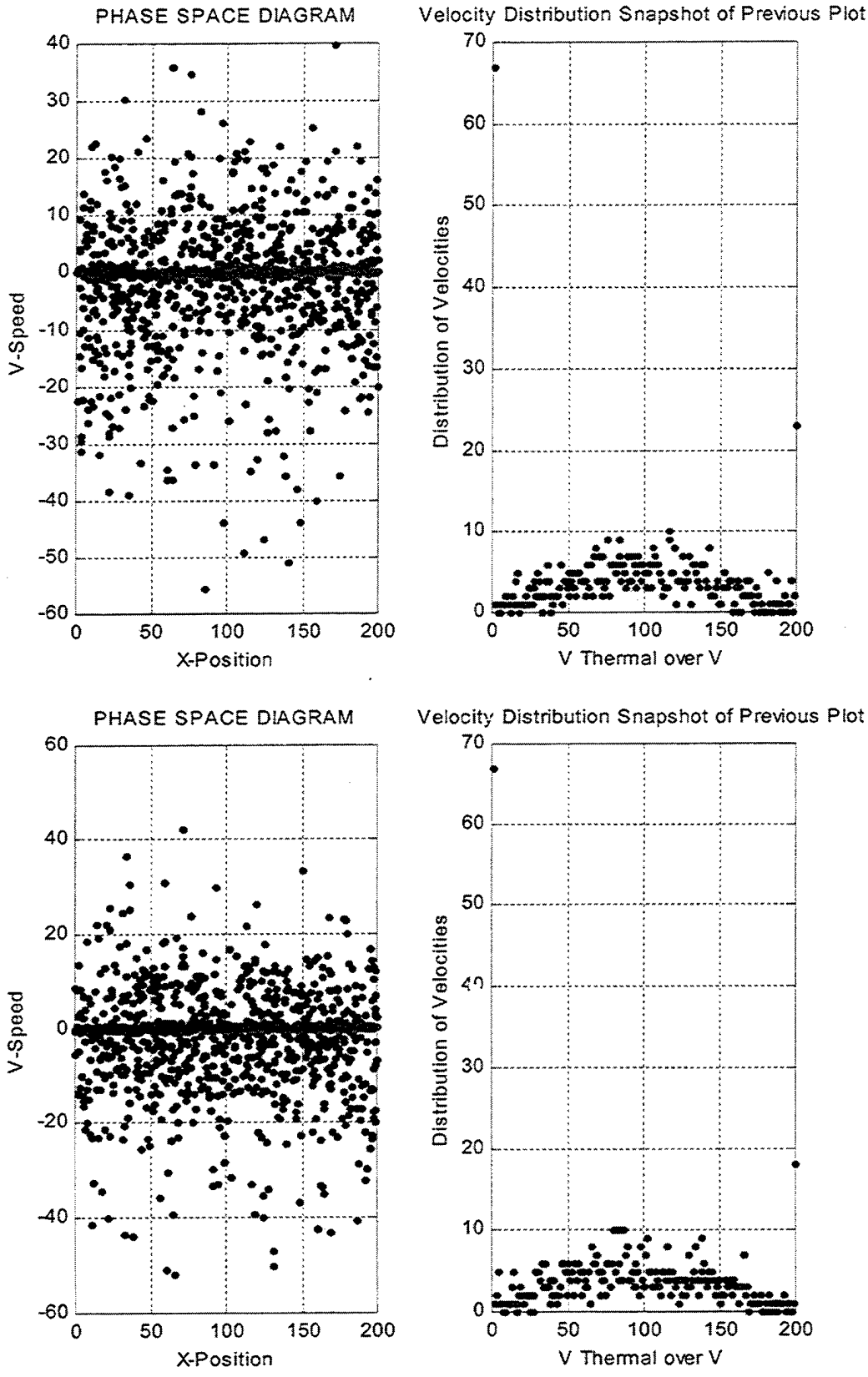

Figures 6s and 6t. Phase Space and Velocity Distributions at times 950 and 1000

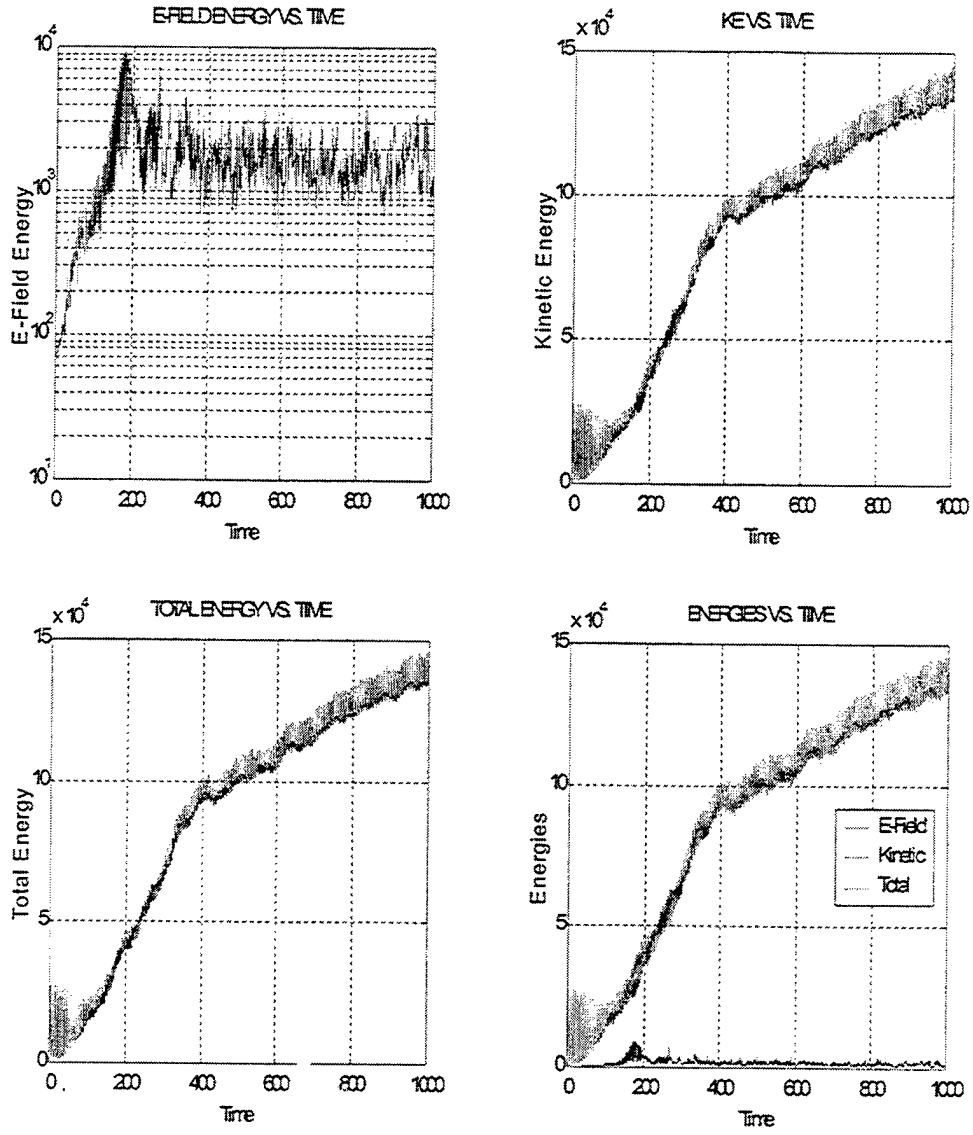

Figure 6u. Energy Plots from time = 0 to time = 1000 / ω_{PLASMA}.

Table 1. Values used for Figures 6a through 6u.

Number of Particles:	1500	Time step:	0.1 / ω_{PLASMA}
Run Time:	1000 time steps	Time Between Plots:	50 / ω_{PLASMA}
Number of Cells:	200	Thermal Electron Velocity:	1

III. INTERPRETATION OF MATLAB RESULTS

Figures 6a through 6t show how the plasma's phase space evolves in time and how the velocity distributions evolve. Each pair of figures is a snapshot of the plasma after 50 time steps; therefore; figures 6a and 6b show the plasma 50 time steps into the run, figures 6c and 6d show the plasma 100 time steps into the run, etc. By examining the phase space distributions, it becomes clear that the oscillating electric field (emulating a laser) is causing ion and electron fluctuations plus electron plasma waves. As the field drives the plasma waves to large amplitudes, the electrons are heated. As time evolves more energy is deposited into the plasma and the electrons are heated to higher and higher temperatures.

Figure 6u is perhaps the most important of all. This series of four individual graphs demonstrates how the energy from the laser is converted to heating in the plasma. The electric field energy exponentiates from 70 to 10,000 within 190 / ω_{PLASMA}, which gives a growth rate of about 0.01 ω_{PLASMA} for the electric field. At around time step 190, the electric field is saturated and can be treated as nearly constant. The kinetic energy of the particles goes from 0 to 100,000 in approximately 400 / ω_{PLASMA}. At time step 400 / ω_{PLASMA}, the kinetic energy's rate of change decreases, and between time steps 400 / ω_{PLASMA} and 1000 /ω_{PLASMA}, the kinetic energy increases from 100,000 to about 145,000 respectively, leading to an energy doubling time of about 1200 / ω_{PLASMA}. The graph of the total energy is a compilation of the two energies, which is then the total energy of the system. The final graph is a pictorial of the

individual energies and their sum. The velocity distributions show that many electrons achieve a higher velocity as time progresses.

IV. SIMULATIONS USING TURBOWAVE

Turbowave is a parallel, three-dimensional, relativistic electromagnetic, particle-in-cell program that uses C++ to simulate plasmas. The code was written by Dan Gordon, Ph.D., UCLA, in 1999. It can simulate plasmas in one, two, or three dimensions. This program is far more useful than MATLAB, and overcomes MATLAB's shortcomings in many respects. Turbowave is resource intensive, but the resulting graphs and movies more than make up for the time tradeoff. The program is written for the Macintosh platform of computers, which makes it difficult for non-Macintosh users to employ the program. The program allows for a far greater number of particles, which dramatically increases the statistical reliability of the simulation, and the program allows for longer simulation times than is realistically possible using MATLAB. Turbowave has more diagnostic tools as well, which means that more information can be garnished from a single simulation. In the simulations that follow, I employ the following diagnostics: Kinetic Energy, Lost Particles, Field Energy, Left Poynting Flux (from the laser as it enters the plasma), Right Poynting Flux (from the laser as it exits the plasma), and Input (from the laser as if no plasma were extant; this is the maximum energy input into the system.

I have used Turbowave to carry out simulations of plasmas to explore the generation of high energy electrons by intense laser light shining on-axis with the simulated plasma. These simulations were motivated by recent experiments carried out by the Atomic Weapons Establishment in which a single beam of 0.53 μm light was shined on a plasma near 0.25 $n_{CRITICAL}$; note that $n_{CRITICAL}$ is the density at which all

incident light striking a plasma is totally reflected. In my simulations, I used a perfectly uniform, collisionless plasma with density $\omega_{PLASMA} / \omega_{LASER} = 1 / 2.1$, which is approximately 0.23 $n_{CRITICAL}$. Note that ω_{LASER} is the angular frequency of the laser, and is equal to $3.556 \cdot 10^{15}$ / second. The plasma lengths used are $(51.2)(c) / \omega_{PLASMA}$ and $(204.8)(c) / \omega_{PLASMA}$, corresponding to 9 microns or 36 microns of plasma, respectively. The 0.53 μm laser light intensity was either $5 \cdot 10^{16}$ Watts / cm^2 or $6 \cdot 10^{15}$ Watts / cm^2. For all the simulations, the laser enters the plasma from the left and propagates to the right. I carried out simulations with and without moving ions in order to clarify the role of ion fluctuations in the generation of high energy electrons.

Most simulations were one-dimensional, allowing variation along the direction in which the laser propagated. A two-dimensional simulation gave quite similar results for the absorption of the laser and heated electron energies. I now will present four simulations using Turbowave.

A. FIXED IONS, "SMALL" PLASMA

In this case, the ions are treated as massive and immovable objects. The characteristics of the set-up include the following parameters:

- $v_{OSCILLATION} / c = 0.1$ (the driver amplitude, related to the dimensionless laser intensity; $v_{OSCILLATION}$ is the electron's velocity as a result of the laser's E-field)
- $\omega_{LASER} / \omega_{PLASMA} = 2.1$
- Plasma length = $(51.2)(c) / \omega_{PLASMA}$
- Duration of the run = $2100 / \omega_{PLASMA}$

Figure 7 shows the evolution in time of various energies for this simulation run. Figure 8 gives the electron energy distribution (number of electrons versus energy) at a time late in the simulation. For this plot, the number of electrons corresponding to a given energy is counted and assigned to a bin.

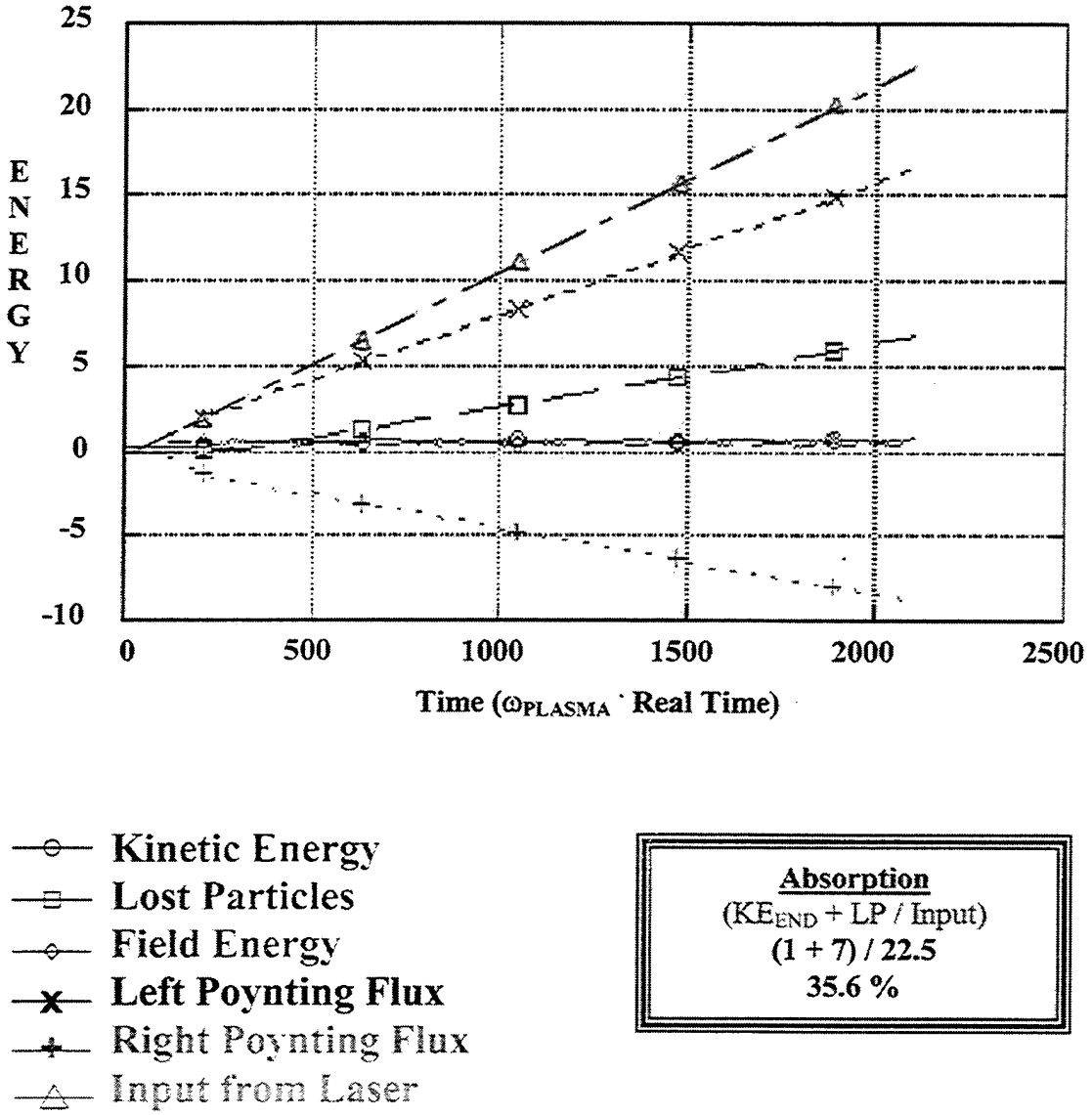

Figure 7. Energy Diagram for Fixed Ions, Small Plasma.

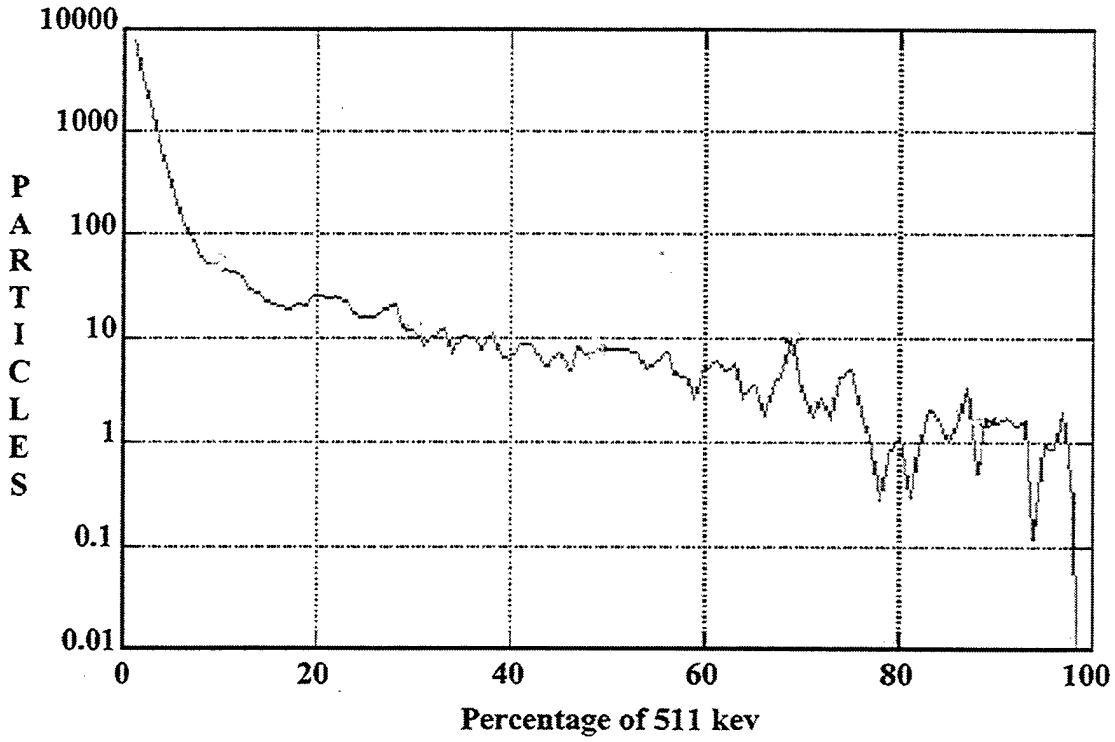

Figure 8. Electron Energy Distribution for Fixed Ions, Small Plasma.

In looking at the energy plots in Figure 7, the laser strikes the plasma from the left and propagates to the right. The initial kinetic energy of the plasma is essentially negligible and can be considered zero. The plasma is driven fairly hard, as is evidenced by a value of 0.1 for $v_{OSCILLATION}$ / c. The length of the plasma is small, only about 9 microns. The ratio of the laser frequency (ω_{LASER}) to the plasma frequency (ω_{PLASMA}) is 2.1, which ensures that the plasma is just below quarter critical density ($0.25 \cdot n_{CRITICAL}$). By the end of the run 2100 / ω_{PLASMA} ($\sim 1.24 \cdot 10^{-12}$ seconds) later, the lost particle energy equates to about 7 (dimensionless units used), and the kinetic energy of the plasma only increases to a value of about 1. Adding these values together and dividing by the input energy (which is the amount of energy crossing the right boundary if there were no

plasma present) from the laser, 22.5, I obtained an absorption value of 0.356. This number equates to the amount of energy absorbed from the laser that is converted to heated electrons.

As shown in Figure 8, the energy distribution consists of a main body that has been heated somewhat from its initial temperature of 2.5 keV plus a tail of higher energy electrons. For the energy range from about 50 keV to 100 keV, the effective plasma temperature is 67 keV. For the higher energies, an effective temperature is 178 keV. These temperatures are roughly those estimated by (m) · (v_{PHASE}^2) / 2, where one uses the phase velocity of the plasma wave associated with the Raman back and forward scattering of the laser light, repectively.

B. FIXED IONS, "LONG" PLASMA

The next simulation has the same parameters, except the intensity is lower and the plasma length is longer. The characteristics of the set-up include the following parameters:

- $v_{OSCILLATION} / c = 0.04$
- $\omega_{LASER} / \omega_{PLASMA} = 2.1$
- Plasma length = $(204.8)(c) / \omega_{PLASMA}$
- Duration of the run = $1400 / \omega_{PLASMA}$

Figure 9 shows the evolution in time of the various energies for this simulation. Figure 10 shows the resulting electron energy distribution for a time late in the simulation.

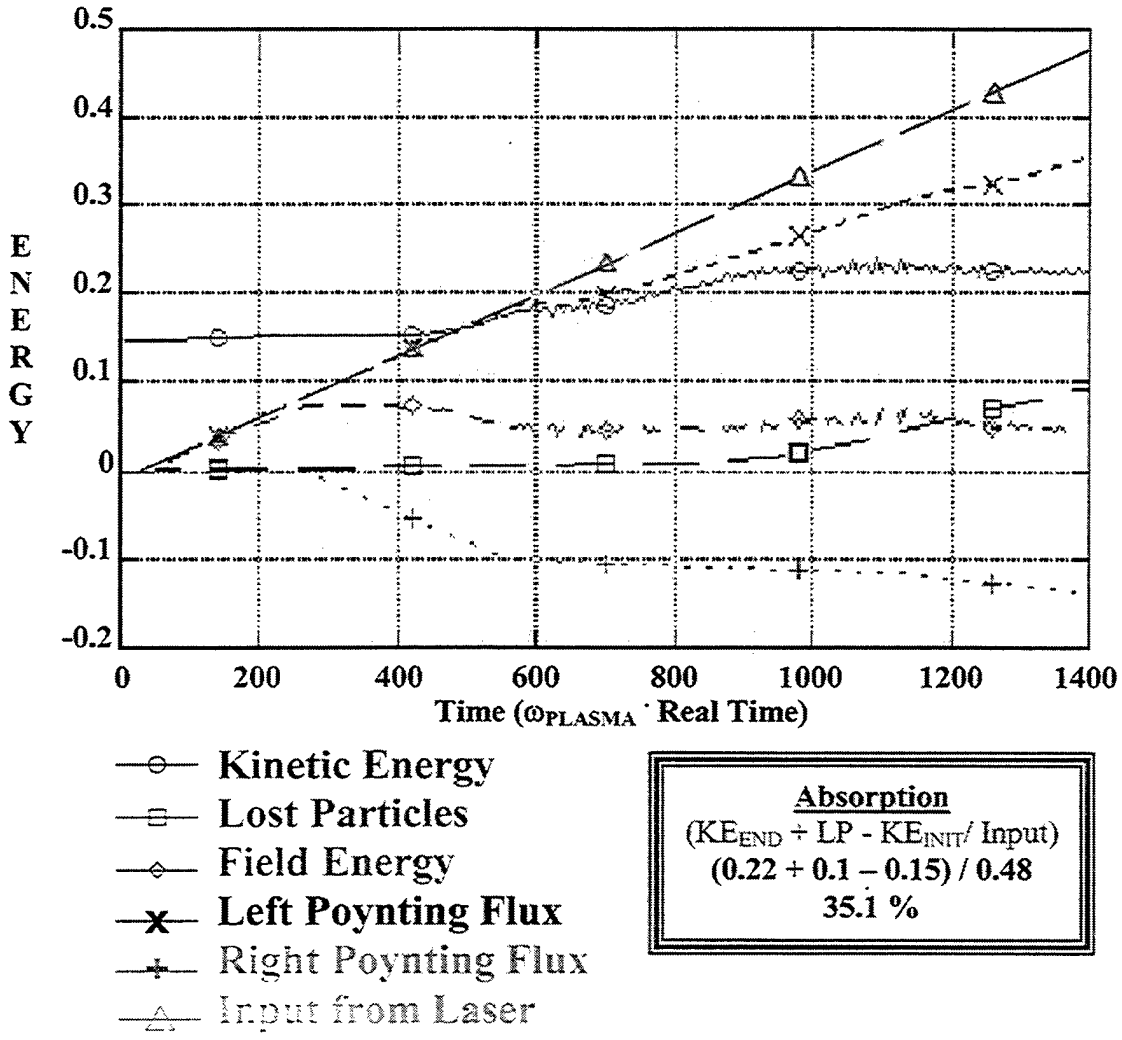

Figure 9. Energy History for Fixed Ions, "Long" Plasma.

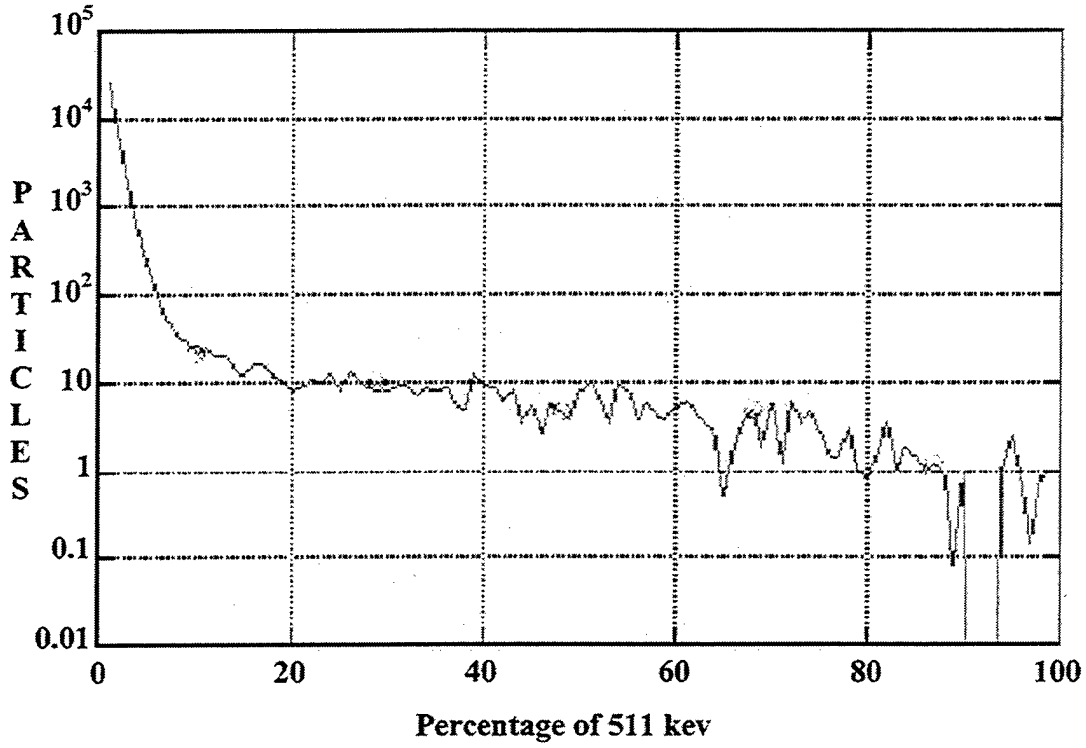

Figure 10. Electron Energy Distribution for Fixed Ions, "Long" Plasma.

The energy plot in Figure 9 again enables one to determine the laser energy absorption. The initial kinetic energy of the plasma is not negligible and is approximately 0.15 (dimensionless units!). The plasma is not driven as hard as in the first case, as is evidenced by a value of 0.04 for $v_{OSCILLATION}$ / c. The length of the plasma is about 36 microns. As before, the ratio of the laser frequency (ω_{LASER}) to the plasma frequency (ω_{PLASMA}) is 2.1, which ensures that the plasma is just below quarter critical density ($0.25 \cdot n_{CRITICAL}$). By the end of the run $1400 / \omega_{PLASMA}$ ($\sim 8.28 \cdot 10^{-13}$ seconds) later, the lost particle energy equates to about 0.1 (dimensionless units used), and the kinetic energy of the plasma only increases to a value of about 0.22. Adding the values of the lost particle energy with the final kinetic energy and subtracting the initial

kinetic energy, and dividing by the input energy from the laser (which is the amount of energy crossing the right boundary if there were no plasma present), 0.48, I obtained an absorption value of 0.351. This number equates to the amount of energy absorbed from the laser that is converted to heated electrons, and is close to the value found in the first case. The plasma is longer but more weakly driven, which leads to about the same amount of absorption.

The energy distribution in Figure 10 again shows a hot main body plus a high energy tail. For the energy range of 50 keV to 100 keV, the heated electron temperature is about 45 keV. For the higher electron energies, the effective temperature is about 135 keV. These values are again quite similar to those found in the smaller, more strongly driven simulation previously discussed.

C. MOVING, DAMPED IONS, "SMALL" PLASMA

In this case, the ions are treated as mobile objects. For simplicity, an ion-electron mass ratio of 100:1 is used. This value is sufficient enough to separate the time scaling for electron and ion motion and enables quicker simulations. The characteristics of the set-up include the following parameters:

- $v_{OSCILLATION} / c = 0.1$
- $\omega_{LASER} / \omega_{PLASMA} = 2.1$
- Plasma length = $(51.2)(c) / \omega_{PLASMA}$
- Duration of the run = 700 time steps

Figure 11 shows the time histories of the various energies for the simulation. Figure 12 shows the electron energy distribution from a time late in the simulation.

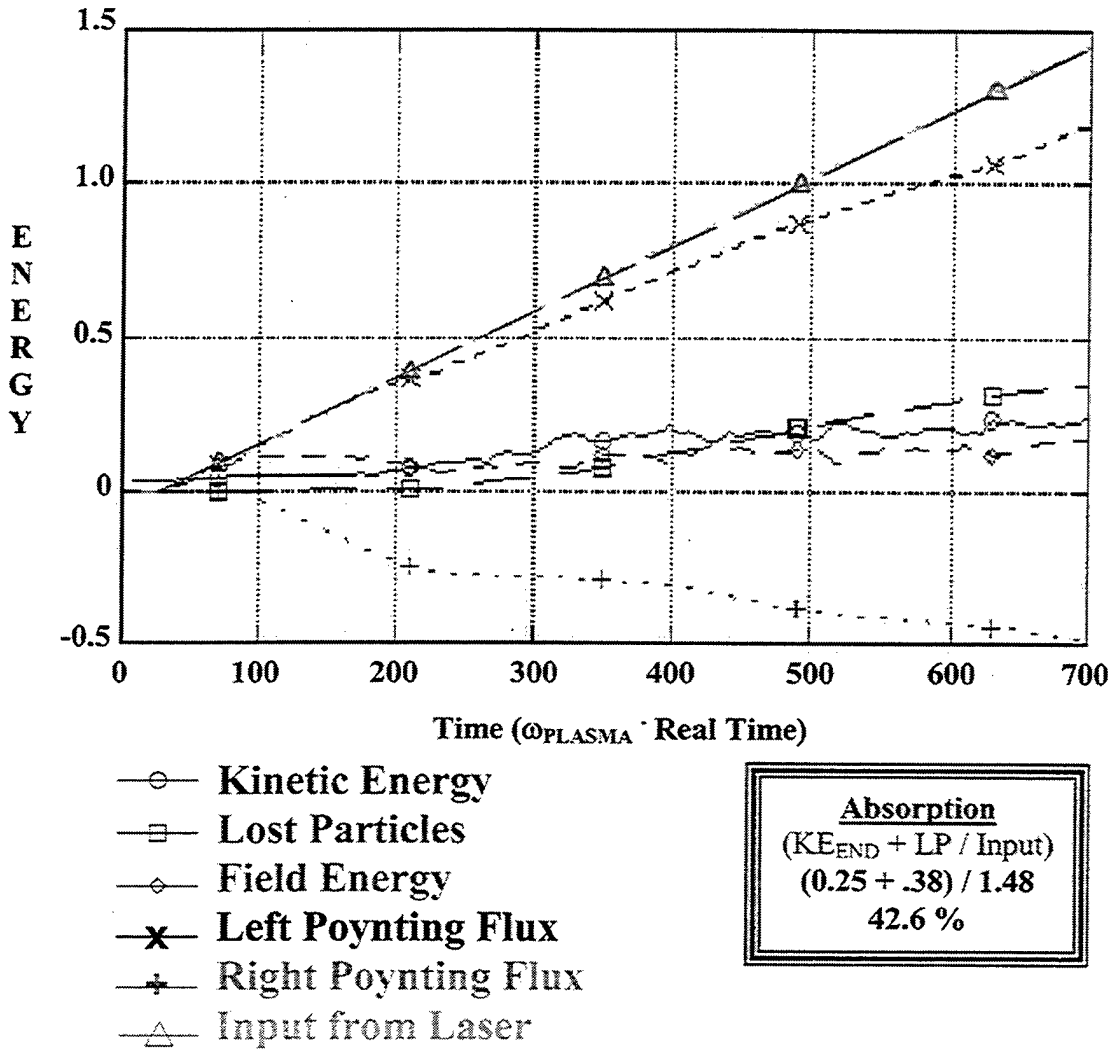

Figure 11. Energy History for Moving, Damped Ions, Small Plasma.

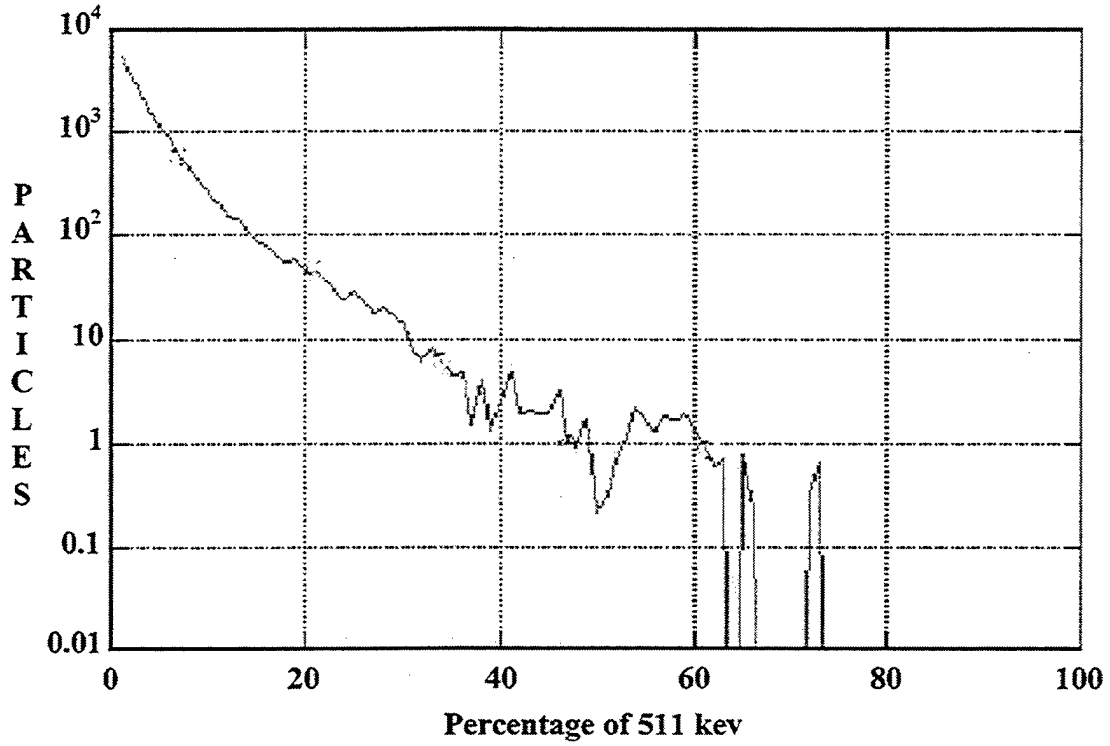

Figure 12. Electron Energy Distribution for Moving, Damped Ions, Small Plasma.

As done with the previous cases, Figure 11 determines the laser absorption. In looking at Figure 11, the laser strikes the plasma from the left and propagates to the right. The initial kinetic energy of the plasma is essentially negligible and can be considered zero. The plasma is driven hard, as is evidenced by a value of 0.1 for $v_{OSCILLATION}$ / c. The length of the plasma is small, only about 9 microns. The ratio of the laser frequency (ω_{LASER}) to the plasma frequency (ω_{PLASMA}) is 2.1, once again ensuring that the plasma is just below quarter critical density ($0.25 \cdot n_{CRITICAL}$). By the end of the run $700 / \omega_{PLASMA}$ ($\sim 4.14 \cdot 10^{-13}$ seconds) later, the lost particle energy equates to about 0.38 (dimensionless units used), and the kinetic energy of the plasma only increases to a value of about 0.25.

Adding these values together and dividing by the input value, 1.48, from the laser (which is the amount of energy crossing the right boundary if there were no plasma present), I obtained a value of 0.426. This number equates to the amount of energy absorbed from the laser that is converted to heated electrons and ions. This absorption is about 20% greater than that found in the previous case involving a small plasma and fixed ions.

One can infer two temperatures from the high energy electrons shown in Figure 12. These temperatures are 33 keV and 90 keV associated with the Raman back scattered and forward scattered light, respectively. Significant ion fluctuations which significantly lowered the heated electron energies developed in this simulation. Note that lower temperature reasonably agrees with the hot electron temperature measured in an actual experiment performed with the Helen Atomic Weapons Establishment 2ω (0.530 μm) green laser in England. The similarities between the computer simulation and the actual experiment show that this technique reproduces observed laser-plasma coupling and other phenomena within a reasonable amount of error.

D. MOVING IONS, "LONG" PLASMA

Once again, the ions are treated as massive and mobile objects. The simulation parameters are similar to the ones found in the third case (moving, damped ions, small plasma). The characteristics of the program's input variables include the following parameters:

- $v_{OSCILLATION} / c = 0.04$
- $\omega_{LASER} / \omega_{PLASMA} = 2.1$

- Plasma length = (204.8)(c) / ω_{PLASMA}
- Duration of the run = 1400 / ω_{PLASMA}

Figure 13 shows the time evolution of the energies in this simulation, and Figure 14 shows the electron energy distribution at a time late in the simulation.

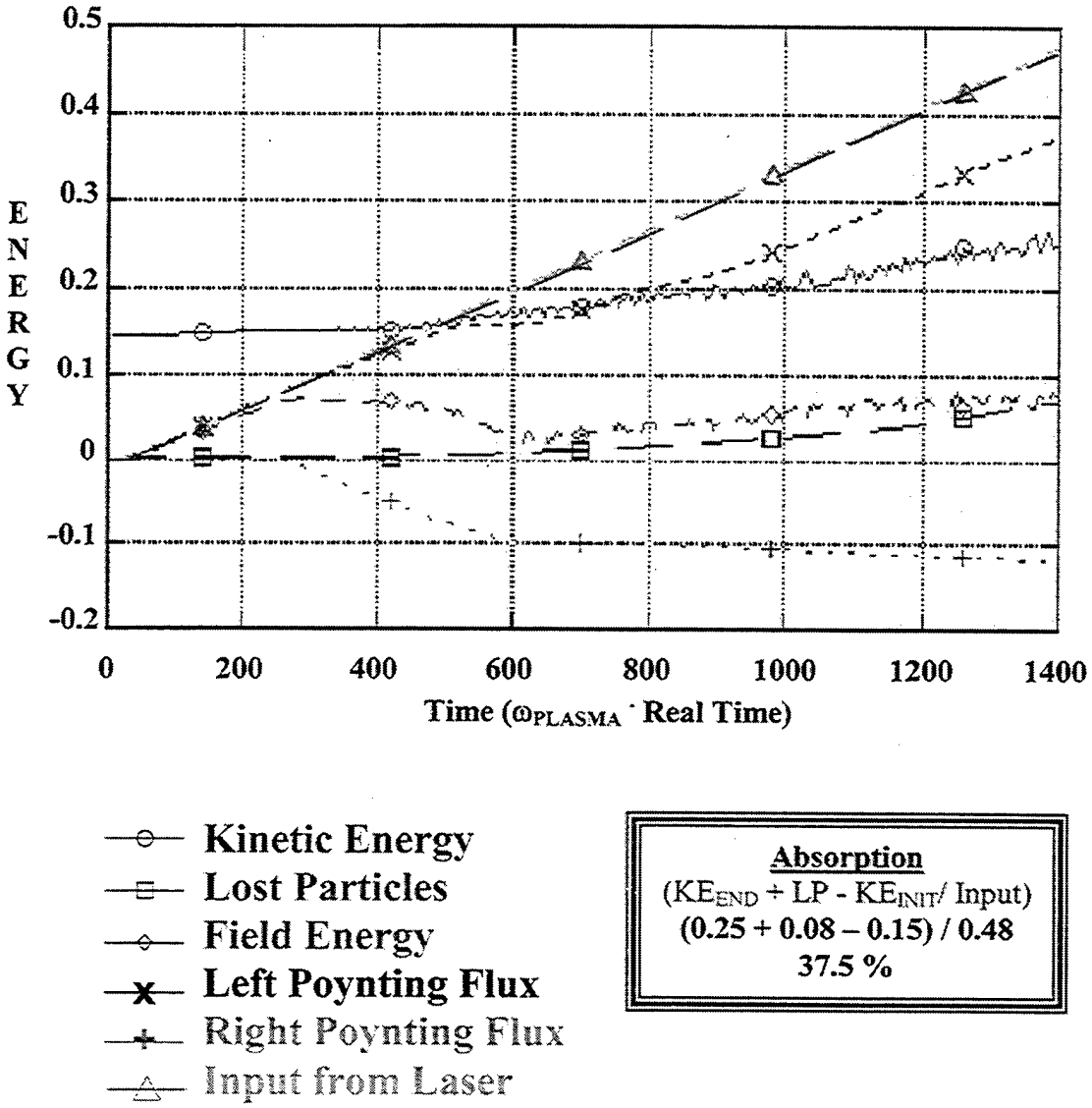

Figure 13. Energy History for Moving Ions, "Long" Plasma.

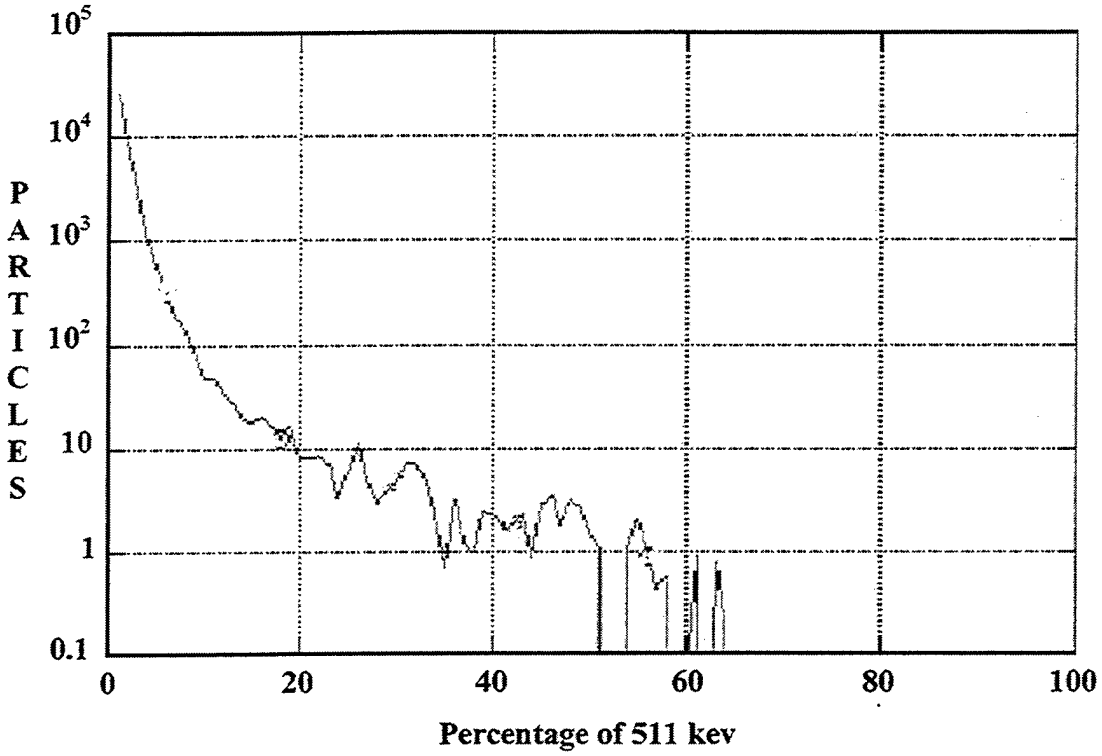

Figure 14. Distribution Versus Energy Plot for Moving Ions, "Long" Plasma.

Since the ions are moving, ion fluctuations again develop. In looking at Figure 13, the laser strikes the plasma from the left and propagates to the right. The initial kinetic energy of the plasma is not negligible and is about 0.15 (dimensionless units!). The plasma is not driven very hard, as is evidenced by a value of 0.04 for $v_{OSCILLATION} / c$. The length of the plasma is large, about 60 wavelengths of light. The ratio of the laser frequency (ω_{LASER}) to the plasma frequency (ω_{PLASMA}) is 2.1, which ensures that the plasma is just below quarter critical density ($0.25 \cdot n_{CRITICAL}$). By the end of the run, $1400 / \omega_{PLASMA}$ ($\sim 8.28 \cdot 10^{-13}$ seconds) later, the lost particle energy equates to about 0.08 (dimensionless units used), and the kinetic energy of the plasma only increases to a

value of about 0.25. Adding these values together and dividing by the input value, 0.48, from the laser (which is the amount of energy crossing the right boundary if there were no plasma present), I obtained a value of 0.375. This number equates to the amount of energy absorbed from the laser that is converted to heated electrons and ions. This fraction is nearly the same as that found in the second case with fixed ions.

The temperatures inferred from Figure 14 are now 28 keV and 80 keV for the Raman backscattered and forward scattered light, respectively. These temperatures are again lower than in the fixed ion run and are about the same as those found in the more strongly driven, smaller plasma simulation with moving ions (Case C, "Moving, Damped Ions, Small Plasma"). The lower temperatures compare favorably with those found in the Atomic Weapons Establishment experiment [Reference 5].

V. INTERPRETATION OF ONE DIMENSIONAL TURBOWAVE RESULTS

Each of the above paragraphs contained a specific run with specified constants. It is unfortunate for the reader not to be able to see the accompanying Quick Time movies for each of the runs; the compiled movies of the laser entering the plasma are all quite fascinating. Turbowave generated movies for the laser and scattered light waves, the electric field of the plasma wave, the magnetic fields generated by the laser and the moving plasma charges, and the phase space (heating) of the plasma. The resulting output files were all fairly large, between 500 kilobytes and 15 megabytes in size, and provided a clear picture of what occurs in a uniform, collisionless plasma.

THIS PAGE INTENTIONALLY LEFT BLANK

VI. TURBOWAVE TWO DIMENSIONAL RESULTS

Turbowave was written to handle one, two, and three dimensional analyses of plasmas. Having spent some time on the one-dimensional case, I turned my attention to using Turbowave to illustrate a two-dimensional plasma. Specifically, I was curious to see if the results were comparable. I shall elucidate those results now by providing a single representative study out of several two-dimensional cases that I pursued.

The plasma is allowed to vary in both the x-direction (the direction in which the laser propagates) and in the y-direction. For this simulation, the electric vector of the laser light is in the z-direction. Future simulations will have the electric vector in the y-direction which will then allow the inclusion of the two-plasmon decay instability. The parameters are identical to those found in the third case (Moving, Damped Ions, Small Plasma), except that the simulation is two-dimensional. The characteristics of the program's input deck included the following parameters:

- $v_{OSCILLATION} / c = 0.1$
- $\omega_{LASER} / \omega_{PLASMA} = 2.1$
- Plasma length = (51.2)(c) / ω_{PLASMA} in the x-direction
- Plasma length = (12.6)(c) / ω_{PLASMA} in the y-direction
- Duration of the run = 700 / ω_{PLASMA}
- $T_{ION} / T_{ELECTRON}$ (Temperature) Ratio (for Landau Damping Effects): 1 / 4

Figure 15 shows the history of the various energies in this simulation run. Figure 16 gives the electron energy distribution at a late time in the simulation.

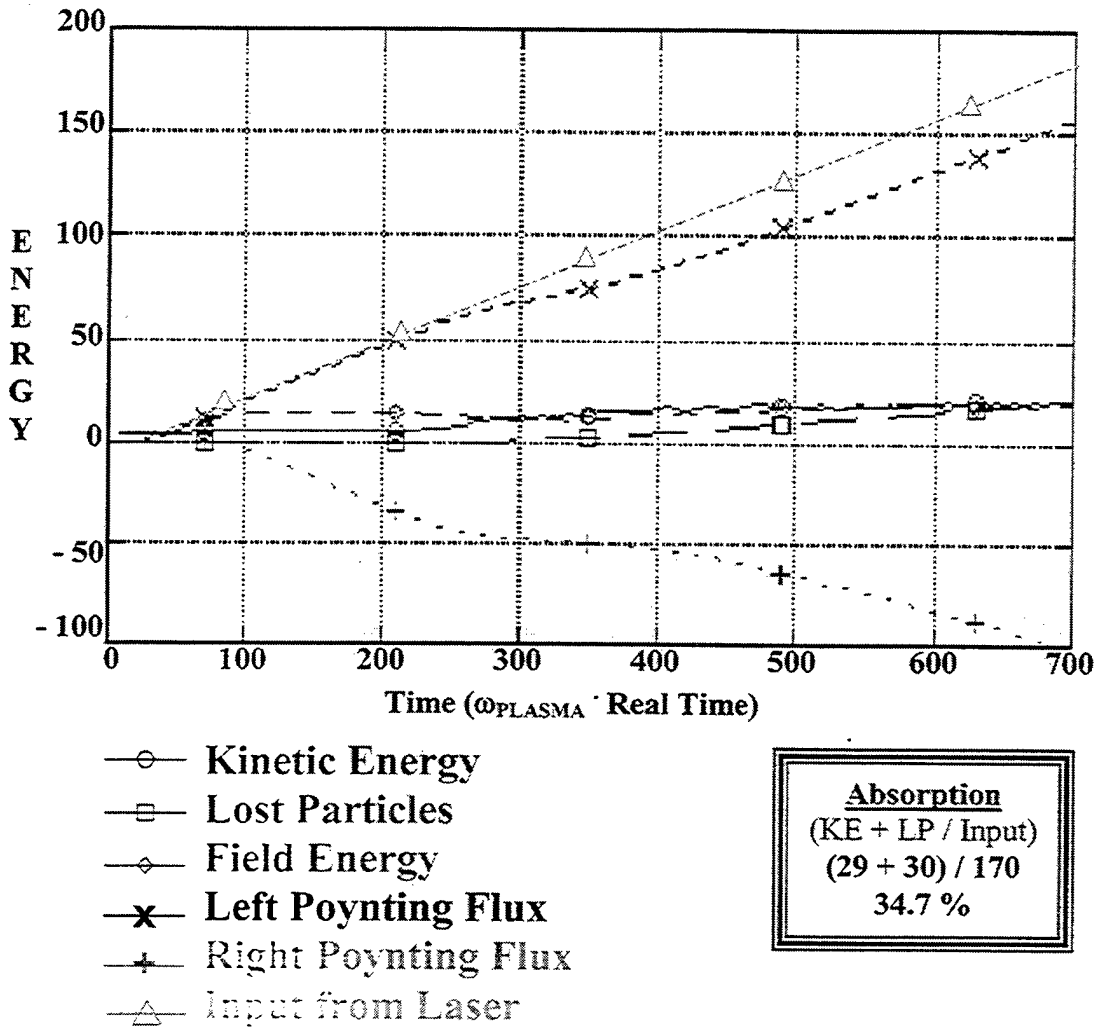

Figure 15. Energy History for Two-Dimensional Turbowave Problem.

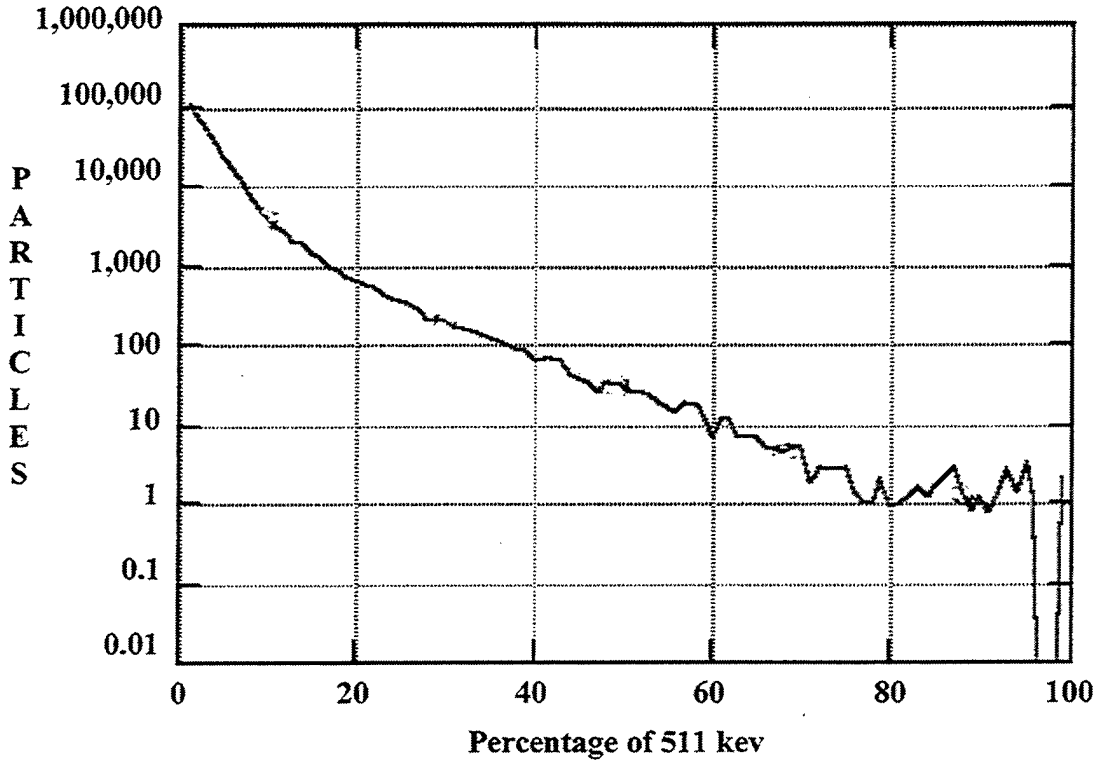

Figure 16. Number of Particles Versus Energy for the 2-D Simulation.

The initial kinetic energy of the plasma is negligible and can be considered approximately zero. The plasma is driven fairly hard, as is evidenced by a value of 0.1 for $v_{OSCILLATION}$ / c. The length of the plasma is small, about 9 microns. The ratio of the laser frequency (ω_{LASER}) to the plasma frequency (ω_{PLASMA}) is 2.1, which ensures that the plasma is just below quarter critical density ($0.25 \cdot n_{CRITICAL}$). By the end of the run $700 / \omega_{PLASMA}$ ($\sim 4.14 \cdot 10^{-13}$ seconds) later, the lost particle energy equates to about 29 (dimensionless units used), and the kinetic energy of the plasma only increases to a value of 30. Adding these values together and dividing by the input value, 170, from the laser input, I obtained an absorption of 0.347 of the laser energy, which is roughly the same value found in the third case (Moving, Damped Ions, Small Plasma) of the one-dimensional simulations. From Figure 16, one infers heated electron temperatures of 36

keV and 60 keV. These temperatures are similar to those obtained from the one-dimensional simulation, although the higher electron temperature is somewhat less (60 keV versus 90 keV). Significant fluctuations in the ion density have again occurred in the two-dimensional simulation.

These results compare favorably with the one-dimensional simulation, including the amount of energy converted from the laser light into heated electrons and ions. T_{HOT} is nearly equivalent for both cases, so it appears that you don't improve your results merely by adding another dimension. The one-dimensional results are apparently good enough. It should be noted as well that the time to execute a two dimensional simulation is much greater than that of the one-dimensional case. The majority of the one-dimensional runs were under a few hours of computer computation time, whereas the two dimensional runs required over ten hours to complete.

VII. ANALYSIS OF AN ACTUAL EXPERIMENT WITH THE HELEN LASER

In late 2000, a team of physicists at the Atomic Weapons Establishment in England used the green 0.53 μm Helen laser to conduct a series of experiments in which a single beam of laser light was shot at gold cylinders that were filled with C_5H_{12} gas in which the pressure ranged from 0.4 atmospheres to 1.2 atmospheres. The hohlraum's dimensions were 564 μm by 564 μm, and the cylinder was capped on both ends with polyimide windows that were 3500 Angstroms ($3.5 \cdot 10^{-7}$ m) thick. The polyimide was fully transparent to the green laser light, which ensured that all of the laser's energy was able to pass through and strike the inner wall of the hohlraum. Smoothed beams of intensity $4 \cdot 10^{14}$ Watts / cm^2 and unsmoothed beams of intensity $6 \cdot 10^{15}$ Watts / cm^2 were used. The resulting plasmas ranged from 0.1 $n_{CRITICAL}$ to 0.3 $n_{CRITICAL}$ [Reference 5].

Figure 17 shows the fraction of the laser energy absorbed into high energy electrons versus plasma density normalized to the critical density. Figure 17 shows the results for a series of experiments, but the most relevant data for my simulations are the ones with values near 0.25 $n_{CRITICAL}$. With the laser operating at a peak intensity of $6 \cdot 10^{15}$ Watts / cm^2, the laser generated about 17% hot electrons, roughly half of what was seen in my ideal computer simulations. Our simulations begin with a perfect, uniform plasma; the simulated plasma does not contain the density gradients found in a real plasma. The heated electron temperatures inferred from the x-rays also compares reasonably well with the simulations. As shown in Figure 18, a hot electron temperature

of about 30 keV was observed. It would be interesting to look for the higher energy electron temperature also seen in the simulations.

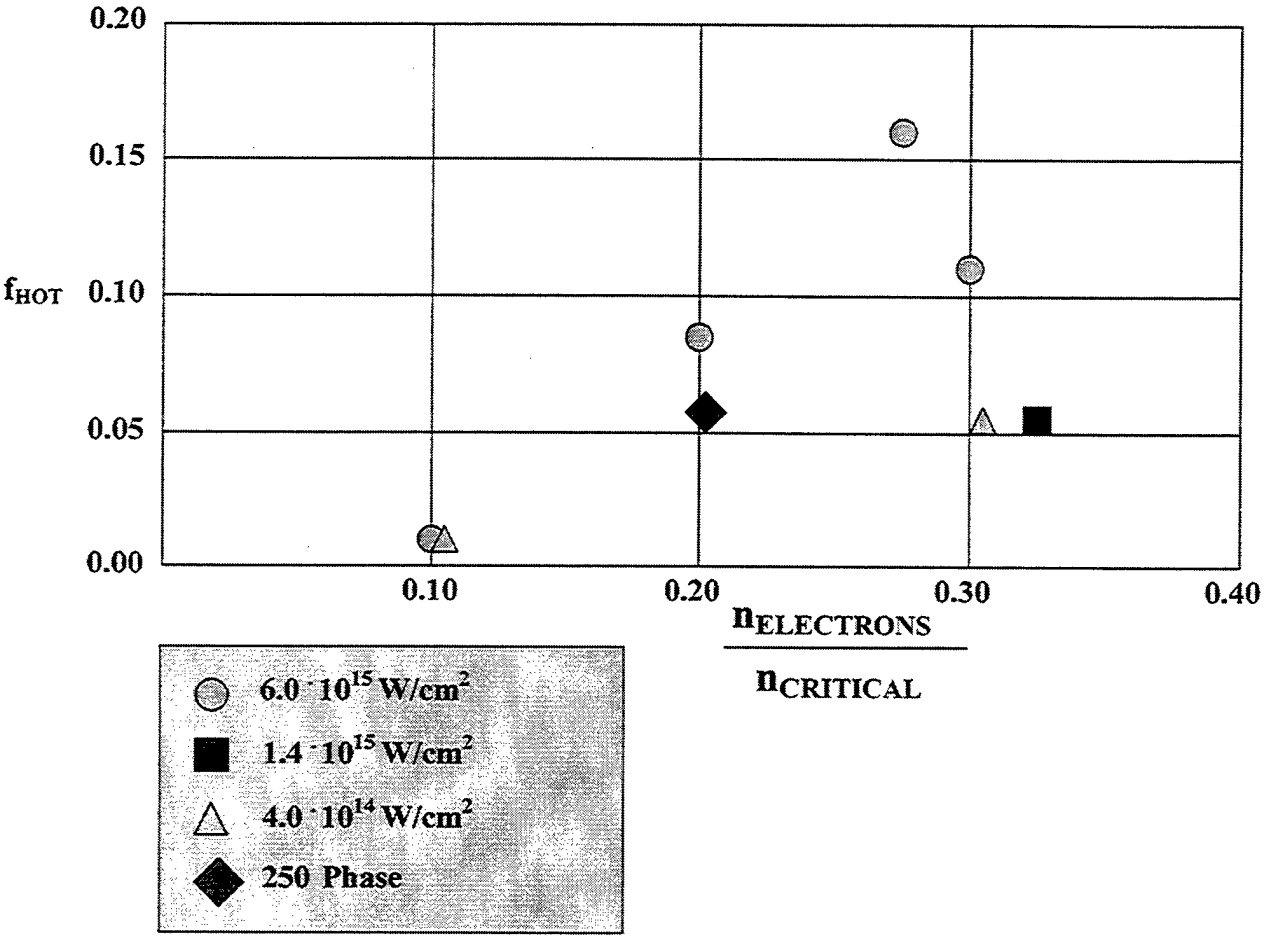

Figure 17. Hot Electron Fraction, f_{HOT}, versus Density. Helen Laser Experiment, Atomic Weapons Establishment, England [Reference 5].

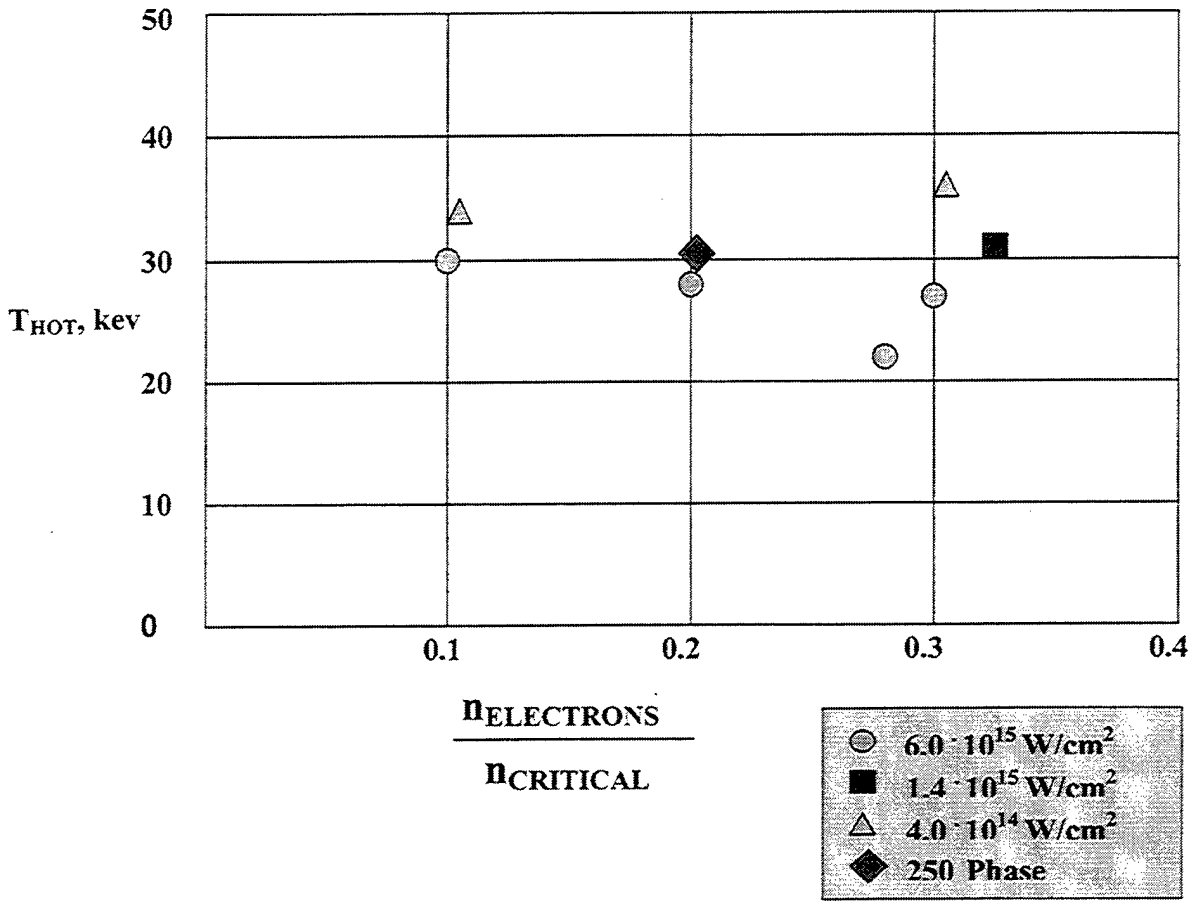

Figure 18. Measured Experimental Values for T_{HOT} Electrons [Reference 5].

THIS PAGE INTENTIONALLY LEFT BLANK

VIII. CONCLUSIONS

This research was motivated by the potential use of 0.53 μm laser light to produce a high-energy x-ray source. This application requires the efficient generation of high-energy electrons which can subsequently produce high-energy x-rays as they transport into a gold or other high-Z wall.

I used one-and two-dimensional computer simulations to explore high-energy electron generation by intense 0.53 μm laser light in a plasma near 0.25 $n_{CRITICAL}$. Simulations with two different laser intensities and plasma lengths showed that a significant amount of the laser's energy is absorbed into high-energy electrons can occur. Ion density fluctuations that develop in the plasma reduce the heated electron temperatures.

The simulations are consistent with some recent experiments at the Atomic Weapons Establishment, England, which show nearly 20 per cent absorption of the green laser light into high-energy electrons when a plasma near quarter critical density is irradiated. The measured hot temperature compares favorably with that seen in the simulations.

More detailed comparisons with experiments will require simulations with a density gradient in the plasma. More two-dimensional simulations are also needed, especially to explore the contribution of the two-plasmon decay instability. Exploration of a variety of boundary conditions for the light waves and the heated electrons is also needed. Finally, it would be valuable to carry out simulations with lower laser intensities closer to those used for laser fusion applications.

No doubt that Turbowave is useful to predict plasma behavior for lasers of any intensity and wavelength. Further research could include using the code to determine the viability of fusion at lower laser intensities. It is well known that higher intensities produce high-energy electrons and x-rays; for fusion to occur, one would want to limit the production of both. In this thesis, I wanted to produce high-energy electrons and x-rays, so I deliberately kept the intensities high.

I hope that this paper will assist further research into the viability of using green laser light over more damaging blue; although not addressed, it has been shown that green laser light causes far less damage in the optics assemblies because the energy deposited is significantly less than when blue light is used. Green light might very well be a useful option for the National Ignition Facility and elsewhere for a myriad of advanced applications, including sustained fusion.

Finally, the one-dimensional MATLAB code was a useful introduction to the basic steps of computer simulation. However, I found that this code was insufficient to execute the task of simulating a large-scale plasma with a large number of particles. The MATLAB run depicted here required a tremendous amount of RAM (384 Megabytes), and the simulation took more than 10 hours. The total number of particles involved was a scant 1500, versus the 80,000 to 100,000 typically used in Turbowave. Plotting the results in MATLAB were not nearly as illustrative as in Turbowave, and the option to do a movie in MATLAB was attempted with very disappointing results. Even with the large quantity of memory available, the computer could not handle the graphics. Turbowave, on the other hand, attacked the problem with elegance and grace. Its only drawback was that it was written for the Apple Macintosh platform, although it can be modified to run

on IBM PCs with some effort. All of the resulting graphs and movies had to be converted to PC format in order to be genuinely useful, and that took a great deal of time to execute. I can't recommend studies in MATLAB unless the user desires to deal with very small plasmas and short timesclaes. Turbowave is by far the better choice to handle this kind of problem.

THIS PAGE INTENTIONALLY LEFT BLANK

LIST OF REFERENCES

1. Kruer, William L., *Physics of Laser Plasma Interactions*, (Addison-Wesley), Redwood City, 1988

2. Chen, Francis F., Introduction to Plasma Physics and Controlled Fusion Vol I, (Plenum Press), New York, NY 1984

3. Birdsall, C. K., and Langdon, A. B., Plasma Physics via Computer Simulation, Institute of Physics Publishing, Philadelphia, PA, 1998

4. Pärt-Enander, Eva, Sjöberg, Anders, Melin, Bo, and Isaksson, Pernilla, The MATLAB Handbook, (Addison-Wesley), Menlo Park, CA, 1996

5. Stevenson, M., et al., paper O1-4, Suter, L., paper P1-9, 31st Conference on Anomalous Absorption of Radiation in Plasmas (June 3 – 8, 2001)

6. Jones, W. David, et al., paper P2-3, 31st Conference on Anomalous Absorption of Radiation in Plasmas (June 3 – 8, 2001)

7. Gordon, Daniel, et al., IEEE Trans. Plasma Sci. 28, 1224 (2000)

THIS PAGE INTENTIONALLY LEFT BLANK

INITIAL DISTRIBUTION LIST

1. Defense Technical Information Center 2
   8725 John J. Kingman Road, Suite 0944
   Ft. Belvoir, VA 22060-6218

2. Dudley Knox Library 2
   Naval Postgraduate School
   411 Dyer Road
   Monterey, CA 93943-5101

3. Engineering and Technology Curricular Office, Code 34 1
   Naval Postgraduate School
   Monterey, CA 93943

4. Department of Physics 2
   United States Military Academy
   West Point, New York 10996
   Attention: COL Winkel

5. Chairman, Department of Physics 2
   Naval Postgraduate School
   Monterey, CA 93943

6. Professor William L. Kruer, Code PH/Kw 1
   Naval Postgraduate School
   Monterey, CA 93943

7. Professor William B. Colson, Code PH/Cw 1
   Naval Postgraduate School
   Monterey, CA 93943

8. Captain W. David Jones 5
   PO Box 98
   West Point, NY 10996

9. Defense Threat Reduction Agency 1
   8275 John J. Kingman Road
   MSC 6201
   Fort Belvoir, VA 22060-6201